THE UNIVERSITY OF ALBERTA

DELAYED RECTIFICATION IN FROG ATRIAL MUSCLE

by

© WAYNE RODNEY GILES

A THESIS

SUBMITTED TO THE FACULTY OF GRADUATE STUDIES

IN PARTIAL FULFILMENT OF THE REQUIREMENTS FOR THE DEGREE

OF MASTER OF SCIENCE

DEPARTMENT OF PHYSIOLOGY

EDMONTON, ALBERTA

FALL, 1970

UNIVERSITY OF ALBERTA

FACULTY OF GRADUATE STUDIES

The undersigned certify that they have read, and recommend to the Faculty of Graduate Studies for acceptance, a thesis entitled

"Delayed Rectification in Frog Atrial Muscle. A Partial Analysis of the Non-specific Ionic Currents Recorded from Atrial Trabeculae of Rana catesbeiana"

submitted by WAYNE RODNEY GILES in partial fulfilment of the requirements for the degree of Master of Science.

ABSTRACT

1. A double sucrose gap technique has been used to polarize and voltage clamp muscle strips from the atrium of the American bullfrog, Rana catesbeiana.
2. In response to steady depolarizing currents, normally quiescent muscle strips frequently show pacemaker activity, and a prolonged depolarization may occur after the stimulus is terminated.
3. Voltage clamp experiments were done in order to investigate the properties of the outward membrane currents which underlie the observed delayed rectification and pacemaker activity.
4. At holding potentials of -30 or -40 mV. relatively short depolarizing voltage clamp pulses activate two distinct current components. On return to the holding potential, the decay of these currents produces a positive tail. Semilog analysis of these tails, reveals the presence of two current components having markedly different time constants of decay. The time constant of the faster component is of the order of 100 to 500 msec., while that of the slower component is approximately 1.5 to 2.1 seconds.
5. Very short duration voltage clamp pulses (less than 1 sec.) activate only the slowly decaying component of outward current. However, during longer clamp pulses, both current components are invariably activated.

6. Experiments designed to determine the reversal potential of these current components show that the slower component reverses at approximately -40 or -50 mV, whereas the faster component reverses at much more negative potentials.

7. Long duration or large magnitude depolarizing clamp pulses frequently give rise to the appearance of a third component in the resultant current tails. This component, which generally manifests itself as a negative current, decays much more slowly than either of the positive components. It has been tentatively attributed to a concentration change of potassium ions in the restricted extracellular spaces of atrial tissue. Its presence interferes with any steady state analysis of the conductance mechanisms.

ACKNOWLEDGEMENTS

I am grateful to Dr. M. Schachter for his permission to enter the Honors Program in the Department of Physiology, and for his ready and effective assistance during this research project.

It is impossible for me to express the full measure of my gratitude to Dr. Denis Noble and his wife, Susan. At every stage of this work, they have provided the supervision, assistance, and encouragement that was needed. In particular, Susan Noble and her colleague, Dr. Hilary Brown, were originally responsible for the development of the technique used in these experiments. I was therefore very fortunate to receive Susan's help in applying this technique to a new preparation. My initial research project, therefore, has been an almost ideal one and has left me with a very high regard for both Susan and Denis as scientists, and as people.

I have greatly appreciated the technical assistance of Mr. A. J. Spindler of the Physiological Laboratory in Oxford. Without his quick and skilled efforts in constructing the perfusion baths, the project could not have been completed within one year.

Dr. H. F. Brown and Dr. A. Clark of the Physiological Laboratory in Oxford have given us access to many of their unpublished results. In this way, they have

contributed to the design and interpretation of some of these experiments.

Mr. F. Loeffler, and Mr. K. Burt have made a special effort to produce the illustrations which follow. Similarly, other members of the academic, technical, and supporting staff of the Department of Physiology have been very helpful, when called upon. The cooperation of each of these people has been very much appreciated.

The financial assistance for this work was provided by the Canadian Medical Research Council and the University of Alberta.

Finally, I wish to thank Mrs. Roseanne Tarnowski for her skilled efforts in typing, and retyping, this thesis.

TABLE OF CONTENTS

TABLE OF CONTENTS

LIST OF FIGURES

LIST OF FIGURES

I. INTRODUCTION:

One of the most striking features of the electrical activity in cardiac muscle is the slow diastolic depolarization, or pacemaker potential. In order to analyse the ionic current changes which give rise to the pacemaker potential, it is necessary to accurately control the membrane potential. This kind of control became possible with the invention of the voltage clamp technique (Cole, 1949; Marmont, 1949), but for a long time technical difficulties restricted its application to nerve.

In the case of heart muscle, the anatomical features and contractile properties make the voltage clamp technique very difficult to apply. In fact, the first voltage clamp studies were not reported until 1964 when Deck, Kern and Trautwein; and Hecht, Hutter, and Lywood successfully clamped a short Purkinje fibre preparation. More recently, Noble and Tsien (1968) have done a quantitative analysis of the membrane current which underlies the pacemaker potential in the Purkinje fibre. This, and later studies (Noble and Tsien, 1969a, and 1969b) have focussed attention on the complexity and functional significance of the delayed outward currents in cardiac muscle. In particular, it was found that the pacemaker depolarization could be attributed to the decline of a slow outward potassium current (i_{K_2}) in combination with a maintained inward current.

The natural pacemaker of the heart, however, is in the sinus region. It is therefore important to investigate the possibility that certain features of the ionic currents which generate the natural pacemaker may differ from those observed in the Purkinje fibre. At present, the technical difficulties involved in voltage clamping the sinus have not been solved. However, in many ways the electrical properties of the atrium closely resemble those of the sinus.

Hence, Brown and Noble (1969a,b), using a double sucrose gap technique, began a voltage clamp analysis of the outward current changes in the atrium of the Hungarian bullfrog, Rana ridibunda. Their initial results, although incomplete, indicated that a pacemaker mechanism can be induced in the atrium which differs in several important ways from that of the Purkinje fibre.

This series of experiments were designed to extend these findings. Its objectives were:

1. To confirm the existence of currents identified by Brown and Noble in a new preparation, Rana catesbeiana.
2. To further analyse the slow current changes, in an attempt to determine the ionic basis for the pacemaker potential, and the repolarization phase of the action potential.

As an introduction to this voltage clamp analysis, it may be useful to review some of the known electrophysiological properties of the atrium, and to give a short description of the double sucrose gap technique.

I.1 IONIC CURRENTS UNDERLYING THE RESTING POTENTIAL:

Experiments designed to measure the potassium and sodium fluxes in quiescent frog atria have helped to identify the steady ionic currents which flow at the resting potential. In this way, Haas, Glitsch and Trautwein (1963) showed that the resting potassium conductance was approximately four times larger than the resting sodium conductance. Therefore, the ratio of extracellular to intracellular potassium ion concentrations would seem to be the main determinant of the resting potential in cardiac muscle (as in nerve and skeletal muscle). Normally, however, the membrane potential is 10 to 20 mV positive to the potassium equilibrium potential (E_K), which is predicted by the Nernst equation. This suggests the presence of a steady, inward current, probably carried by sodium, and perhaps also calcium ions.

When the extracellular potassium ion concentration (K_o) is increased, the membrane potential (E_m) changes by an amount that corresponds quite closely to the depolarization predicted by the Nernst equation. Decreases in K_o, however, do not produce correspondingly large changes in the membrane potential (Luttgau and Niedergerke, 1958; Brady and Woodbury, 1960). This observation also suggests the presence of a significant inward current which prevents the membrane hyperpolarizing towards very negative values of E_k.

Unlike Purkinje fibres, frog atria do not depolarize in potassium-free media. In the Purkinje fibre, this depolarization has been attributed to inward potassium rectification in the presence of a significant resting sodium conductance (Noble, 1965). Since there is good evidence for an appreciable steady sodium conductance in atrial muscle, the absence of depolarization in potassium-free media indicates that (i) the potassium concentration in the extracellular spaces may remain significant, even when K_o is reduced to zero, or (ii) inward rectification is less marked in atrial muscle. The second possibility is unlikely, however, since Haas, Glitsch and Kern (1966) have shown that the potassium conductance, estimated from flux measurements, reaches high values only when the driving force, (E_m-E_k), is directed inwards. Moreover, current-voltage relations obtained from voltage clamp experiments (Brown and Noble, 1969a) show that marked inward rectification is present in frog atria.

Hence, it is more likely that the absence of depolarization in potassium-free media may be attributed to anatomical features which make it difficult to reduce the extracellular potassium concentration to very low values. This could result from the much larger surface to volume ratio in a preparation which is formed by large numbers of small cells. The exchange of intracellular potassium with the extracellular spaces may then be too rapid to allow sufficient time for equilibration with the bathing solution.

If this is the case, then experimental conditions under which large outward currents are produced may cause significant concentration changes in the extracellular spaces of the preparation (see Discussion).

I.2 PASSIVE ELECTRICAL PROPERTIES OF THE ATRIUM:

Anatomically, atrial muscle is composed of discrete cells. Physiologically, however, the entire atrium functions as if it were a single cell. This syncytial behaviour is characteristic of heart muscle, and raises questions regarding the mechanism by which excitatory impulses are conducted from cell to cell.

Barr, Dewey and Berger (1965) have conclusively shown that impulse conduction in the atrium, as in all other excitable tissues, occurs by means of local circuit currents. They found that conduction failed when an 0.5 mm gap perfused with isotonic sucrose separated the two ends of a preparation bathed in normal Ringer's solution. However, bypassing the sucrose gap with a sufficiently low resistance restored conduction. Since the gap width exceeded the atrial cell length, current in one cell must have spread in an electrotonic fashion to adjacent cells.

It should therefore be possible to describe the properties of atrial tissue in terms of conventional cable theory. However, since the atrium does not behave as a simple core conductor, an applied current may spread in a multidimensional fashion from the current source. This

makes cable analysis very difficult to perform and interpret.

Table I summarizes the results of several attempts to quantitatively analyse the membrane properties of heart muscle. Trautwein, Kuffler and Edwards (1956), using fine external electrodes, measured changes in the time course and spatial spread of subthreshold electrotonic potentials applied to frog atrial muscle. On this basis they obtained estimates of the time and space constants of the membrane and calculated the membrane capacitance, the membrane resistance, and the internal resistivity of the myoplasm. Later, Woodbury and Crill (1961) used intracellular microelectrodes to map current spread in sheets of rat atrial muscle. Their experiments showed that the spatial decrement of an applied potential in the atrium was significantly steeper than the exponential decay observed in those excitable tissues which act as a simple cable. Hence, a point source of current is very ineffective as a means of polarizing atrial muscle.

Woodbury and Gordon (1965) have used a suction electrode to apply current to frog atrial trabeculae, in an attempt to obtain only one-dimensional current spread. In this way, they hoped to be able to measure the membrane properties of the atrium sufficiently accurately to construct an equivalent electrical circuit. Their data, however, show a wide range of values for the various cable parameters. Estimates of R_m for toad atrial muscle (Tanaka, 1959) show

CABLE PROPERTIES OF HEART MUSCLE

	λ	τ	R_m	R_i	C_m
	μ	msec	(ohm cm^2)	(ohm cm)	$\mu F/cm^2$
Weidman (1952) - Sheep Purkinje Fibre	1900	19.5	1940	105	12
Trautwein et al. (1956) - Frog Atrium	230-410	3.6-9.8	280	100	30
Tanaka (1959) - Toad Atrium	*	*	2000-8000	*	*
Woodbury & Crill (1962) - Rat Atrium	130-160	*	*	*	*
Woodbury & Gordon (1965) - Frog Atrium	50-400	*	13-100	110-1500	25-80

TABLE 1: The symbols in the column headings have the following meanings: λ, d-c space constant of the membrane; τ, time constant of the membrane; R_m, membrane d-c resistance; R_i, specific resistance of the myoplasm; C_m, membrane capacitance. * The values of these parameters were not given in the corresponding paper.

a similar wide range of values. In fact, they are more comparable to those of the Purkinje fibre (Weidman, 1952) than to those of the frog atrium.

It seems probable that much of this uncertainty and variation is a result of errors in experimental methods, or invalid assumptions in analysis. Therefore, until a more accurate method of analysing the cable properties is developed, the absolute values of the cable parameters, and the equivalent circuit of atrial muscle will remain open questions.

I.3 THE DOUBLE SUCROSE GAP TECHNIQUE:

Most applications of the voltage clamp technique use intracellular microelectrodes to polarize the preparation, and to record its potential changes. However, atrial muscle is poorly suited for microelectrode work. The extremely rapid spatial decrement of a subthreshold stimulus applied from a microelectrode (Woodbury and Crill, 1961) means that a point source of current is not capable of uniformly polarizing atrial muscle. Moreover, the contractile responses of the atrium, and the relatively small size of atrial cells (15μ x 15μ x 200μ) reduce the chances of microelectrodes remaining impaled a sufficiently long time to allow voltage clamp analysis to be completed. Finally, it is frequently not possible to pass large enough currents from a microelectrode to maintain uniform polarization of the preparation when large conductance changes are induced.

For these reasons, extracellular electrodes must be used to voltage clamp atrial muscle. The double sucrose gap technique offers one method of doing this. The principle of this technique is as follows.

The true value of a potential difference between two regions of a biological core conductor may be measured only when there is no current flow between these regions. If an appreciable amount of current does flow in the external medium, then measured potentials are reduced according to the following equation:

$$E = E_m \frac{r_1}{r_1 + r_2}$$

where E is the potential recorded across the external resistance, E_m is the true membrane potential, and r_1 and r_2 represent the longitudinal resistances per unit length of the external and the internal medium, respectively. From this equation it is clear that when the external resistance (r_1) is very large, the short circuiting factor

$$\frac{r_1}{r_1 + r_2}$$

approaches one. Hence, the measured potential closely approximates the actual transmembrane potential.

In the double sucrose gap technique, the preparation is perfused with isotonic sucrose in two separate regions along its length. The sucrose 'gaps' present an

extremely high resistance to extracellular current flow. Therefore, using extracellular electrodes, it is possible to (i) measure the transmembrane potential across either gap, or (ii) inject current into the preparation. A detailed description of the way in which this technique may be used to voltage clamp atrial muscle is given in the METHODS section of this thesis.

Two research groups have succeeded in using the double sucrose gap technique to voltage clamp frog atrial muscle. Thus, Rougier et al (1968,1969) have studied the relationship between inward ionic currents and membrane voltage, and Brown and Noble (1969a,b) have quantitatively analysed the delayed outward currents in frog atria.

I.4 MEMBRANE CURRENTS IN ATRIAL MUSCLE:

(a) CAPACITATIVE CURRENT:

Capacitative transients recorded from frog atrial muscle by Rougier, Vassort and Stampfli (1968) show that the capacitative current decays with a time constant which varies between 0.2 and 4.9 milliseconds. Estimates of the total membrane capacitance in the frog atrium (Table 1) indicate that it could be as much as twice as large as that of the Purkinje fibres. It is possible, however, that both the large membrane capacitance and the wide variations in the time constant of discharge arise from structural features of the preparation. Thus in atrial trabeculae, the total membrane area greatly exceeds that of the surface of the

preparation, since each trabeculum is composed of membrane-bound bundles of muscle fibres. In addition, the number of trabeculae contained in each preparation is variable.

The exact arrangement of the membrane capacitance in relation to the membrane resistance has not been established for frog atrial muscle. However, the variability of the time constants would indicate that it may not be as simple as Rougier et al. (1968) imply.

Nevertheless, since the most rapidly activated outward current analysed in these experiments has a time constant of activation of approximately 150 to 400 milliseconds, it is clear that even the slowest capacitative currents do not influence measurements of delayed outward currents.

I.4 (b) INWARD CURRENTS:

Rougier et al. (1969) have studied the inward ionic currents in frog atrial muscle by altering the external sodium and calcium ion concentrations, and by using pharmacological blocking agents (TTX and Mn^{++}) during voltage clamp experiments. On this basis, they have identified two distinct components of inward membrane current, one of which has a much faster time course than the other.

The faster of the two components inactivates with a time constant of approximately 1 millisecond, and is both time- and voltage-dependent. It is reduced when the external sodium concentration is decreased, and is completely inhibited by TTX (5.0×10^{-7} g/ml.). Therefore, it is

thought to be a purely sodium current. This 'fast component' is activated approximately 20 mV positive to the resting potential (+20 mV since Rougier et al have defined the resting potential to be 0 mV), reaches a maximum at around +50 mV, and reverses between +100 and +110 mV. Therefore, it is possible that this current is responsible for the rapid ascending phase, or 'spike', of the atrial action potential.

The slower component of the inward ionic current is also time- and voltage-dependent, but is inactivated much less rapidly than the fast component. In fact, the time constant of inactivation varies between 10 and 20 milliseconds. This current is not sensitive to TTX, (5.0×10^{-7} g/ml.) but appears to be inhibited by Mn^{++} (1 - 2 mM), and is decreased in magnitude when either the external sodium or calcium concentration is decreased. Hence, Rougier et al maintain that this 'slow component' is carried by both sodium and calcium ions. This current activates at approximately +30 or +40 mV (again with respect to the resting potential which is defined as 0 mV), and reaches a maximum between +70 and +80 mV. Hence, it may generate a second phase of the spike of the action potential, as well as being important in the initial part of the plateau. Brown and Noble (1969a) have suggested that this 'slow', TTX-insensitive current may also be important in the development of the pacemaker potential.

1.4 (c) OUTWARD CURRENTS:

Rougier, Vassort and Stampfli (1968) have also recorded the delayed outward currents in the frog atrium.

Their experiments clearly demonstrated the presence of delayed rectification. The outward current which generates this delayed rectification is activated about 40 mV positive to the resting potential, and is not reduced by TEA (20 mM). Hyperpolarizing clamp pulses from the resting potential, however, produce a current response which is markedly inhibited by TEA. If this response is due to the deactivation of a delayed outward current, then it seems possible that two different components of outward current exist in the frog atrium. Without further voltage clamp experiments, however, it is impossible to determine which ions are involved in the delayed responses, or to establish any relationships between them.

Brown and Noble (1969a,b) have done a more detailed study of the delayed currents in the atrium of Rana ridibunda. On the basis of voltage clamp experiments, they postulate that two distinct components of outward current underlie the delayed rectification. The time constant of decay of the faster component is approximately 500 milliseconds at a holding potential of -90 mV, and its reversal potential is between -40 and -70 mV. The time constant of decay of the second component is approximately ten times slower than that of the faster component, and it reverses at more positive potentials.

Semilog analysis of the decay tails shows that each of the delayed responses follows a simple exponential time course. This suggests that first order kinetics govern

both of these current changes, as has been demonstrated in the case of the delayed responses of the Purkinje fibre (Noble and Tsien, 1969). Additional experiments (unpublished), however, indicate that accumulation of positive ions in the restricted extracellular spaces may have produced errors in the quantitative analysis of the slow response. The experiments described in this thesis were therefore designed to re-analyse the conductance changes underlying the delayed outward currents in the frog atrium.

II. METHODS:

II.1 SOLUTIONS:

Two different types of Ringer's solutions and an isotonic sucrose solution were used in these experiments. All solutions were made from analar-brand chemicals (British Drug Houses) and glass-distilled water. The composition of the normal Ringer's solution was based on a serum analysis of the Hungarian bullfrog Rana ridibunda (Miss R. J. Banister, Oxford University).

Normal Ringer's Solution:

NaCl 90 mM; $NaHCO_3$ 20 mM; KCl 2mM; $MgCl_2$ 1 mM; $CaCl_2$ 1.1 mM; glucose 1 g./litre; saturated with 5% CO_2 in 95% O_2

High-Potassium Ringer's Solution:

KCl 92 mM; $KHCO_3$ 20 mM; $MgCl_2$ 1 mM; $CaCl_2$ 1.1 mM; glucose 1 g./litre; saturated with 5% CO_2 in 95% O_2

Isotonic Sucrose Solution:

Sucrose 73 g./litre; saturated with 100% O_2

II.2 DISSECTION PROCEDURE:

Adult American bullfrogs, Rana catesbeiana, were pithed with a scalpel and pithing needle. The ventral body wall was opened and the sternum removed, exposing the beating heart. The pericardium was removed and the ventricular frenulum cut. This allowed the tip of the ventricle to be lifted, so that the sinus venosus and the two aortae

could be sectioned as far from the heart as possible. The intact, freely beating heart was then rapidly transferred to a series of beakers, each containing normal Ringer's solution. It was left for a short time in each beaker while the blood it contained was exchanged for the bathing solution. Agitation with air bubbles from a Pasteur pipette provided additional help in clearing blood from the cavities of the heart.

The heart was then pinned, ventral side up, to the bottom of a perspex dissection dish containing normal Ringer's solution. The bottom of all dissection dishes were covered with a porous, transparent gel (Sylgard resin; Dow-Corning Corp.). Care was taken to place the pins through the truncus arteriosus and the ventricle only. The remainder of the dissection was done with the aid of a dissecting microscope, (Zeiss-Jena stereomicroscope) at magnifications of approximately 11.0, 15.0 or 25.0.

The atria were isolated from the heart as follows: Initially, an incision was made through the connective tissue which joins the truncus arteriosus and the atria, then a second lateral incision was made across the atrio-ventricular border, freeing both atria from the rest of the heart. The atria were then placed in normal Ringer's solution, which was again agitated to remove any remaining blood.

Next, the atria were pinned with the dorsal side uppermost, to the bottom of a second Ringer-filled perspex

dissection dish. An incision was made along the shortest possible distance from the atrio-ventricular aperture to the entrance of the sinus venosus. This produced two flap-like pieces of atrial wall on the dorsal surface of the preparation. Each of these flaps was opened out and pinned down by placing fine pins through the peripheral connective tissue. The interatrial septum was then dissected away and removed. In this way, almost the entire surface of the inner walls of both atria were exposed.

The inner atrial wall is composed of bundles of muscle fibres, or trabeculae, which are covered by an endocardium (Figure 1). Although most of these trabeculae run at different levels and in different directions, a few are relatively free and nonbranching for distances of several millimeters. They can therefore be dissected away from the atrial wall with comparatively little damage to the tissue.

Before the final dissection was begun, the entire atrial wall was inspected under a microscope in order to locate a region where the trabeculae were of the required length (4-5 mm), and were sufficiently parallel and non-branching (Figure 2). However, no attempt was made to consistently dissect from one particular area of the atrium. After a suitable strip had been chosen, a fine nylon thread was tied around its distal end, which was then detached from the atrial wall. The thread was used to gently lift the trabeculae so that more central connections and branchpoints could be severed. This part of the dissection

FIGURE 1: The endocardial surface of the bullfrog atrium. The wall of the atrium is largely composed of trabeculae. The dark spots are pigment cells. (approximately X 8)

FIGURE 2: Endocardial surface of the atrial wall. The upper trabeculum in the darkened central strip would be a typical experimental preparation. (approximately X 35)

catesbeiana, each bundle of muscle fibres is formed by a small number of muscle cells (5 to 10), which are clustered together and surrounded by a basal lamina, or basement membrane. These fibre bundles form branching strands, but individual cells do not appear to branch. Each cell contains between 1 and 4 myofibrils and is approximately 10 microns in diameter, and 175 to 200 microns in length. No structure completely analogous to the intercalated disc of mammalian cardiac muscle has been found in frog atrial muscle. However, regions of close apposition between membranes are frequently observed along the lateral aspect of adjacent cells. These do not occur in conjunction with the Z-lines and have been named cardiac adhesion plaques, close junctions (Baldwin, 1968) or nexuses (Barr, Dewey and Berger, 1965).

Cross-sections of atrial trabeculae (Baldwin, 1968) clearly show that the extracellular space is very restricted, both (i) within the trabeculae, and (ii) within individual bundles of muscle fibres. This finding supports one of the observations of this study. During a depolarizing voltage clamp pulse which has either a relatively large amplitude or a long duration, the resulting outward ionic current almost certainly causes potassium ions to accumulate in the restricted extracellular spaces. By changing the extracellular potassium ion concentration, this accumulation phenomenon alters the electrochemical potential gradient and therefore alters the voltage dependence of the ionic current flow (See Discussion).

was done with the aid of a pair of finely ground scissor-forceps (watchmaker's forceps whose tips had been sharpened on opposite surfaces) constructed by Mr. A. J. Spindler (Physiological Laboratory, Oxford). When the necessary length of tissue had been freed, a second thread was tied around the extreme central end. The remaining attachments between the strip and the atrial wall were then severed.

II.3 PREPARATION:

The final preparation for these experiments, therefore, consisted of a thin strip of atrial muscle which contained a small number (1 to 4) of trabeculae. In each dissection an attempt was made to ensure that the central portion of the strip should contain only one trabeculum. The preparation was later arranged so that this portion occupied the centre or test compartment of the perfusion bath. In some cases, the arrangement of the atrial wall was such that a single trabeculum could be dissected out for the entire length that was required (4-5 mm). The dimensions of the final preparation were estimated to be approximately 300 microns by 4.5 millimetres (Brown and Noble, 1969a).

Recent electron microscope studies (Barr, Dewey and Berger, 1965; Baldwin, 1968) have yielded detailed information regarding the microstructure of frog atrial muscle. In particular, each trabeculum has been shown to be composed of many small bundles of muscle fibres, with the long axis of each fibre lying parallel to the long axis of the trabeculum. According to Baldwin's work on Rana

II.4 PERFUSION BATH AND APPARATUS:

Using the double sucrose gap technique to either uniformly polarize, or voltage clamp atrial muscle requires a particular type of perfusion apparatus. It is essential that the part of the preparation that is to be voltage clamped be very short (approximately 400 microns in our experiments, see CLAMP UNIFORMITY), and that the preparation is separately perfused in five distinct regions along its length, with no communication between these regions. Therefore, the bath must have tightly fitting partitions, and an extremely narrow centre, or test, compartment.

The perfusion baths used in these experiments were designed by Dr. H. F. Brown and Mrs. S. J. Noble (Brown and Noble, 1969a) and were constructed in perspex by Mr. A. J. Spindler (Physiological Laboratory, Oxford).

Each bath consists of an upper and a lower section, and each section is divided into five compartments by four transverse partitions. The placement of these partitions is a critical factor because:

(1) it determines the widths of the different perfusion regions (Figure 3),

(2) it prevents leakage of the solutions from one compartment to another, since the partitions of the top section are vertically aligned with corresponding ones of the lower section.

The upper and lower sections of each bath are identical except that a semicircular groove (150 microns deep, 300

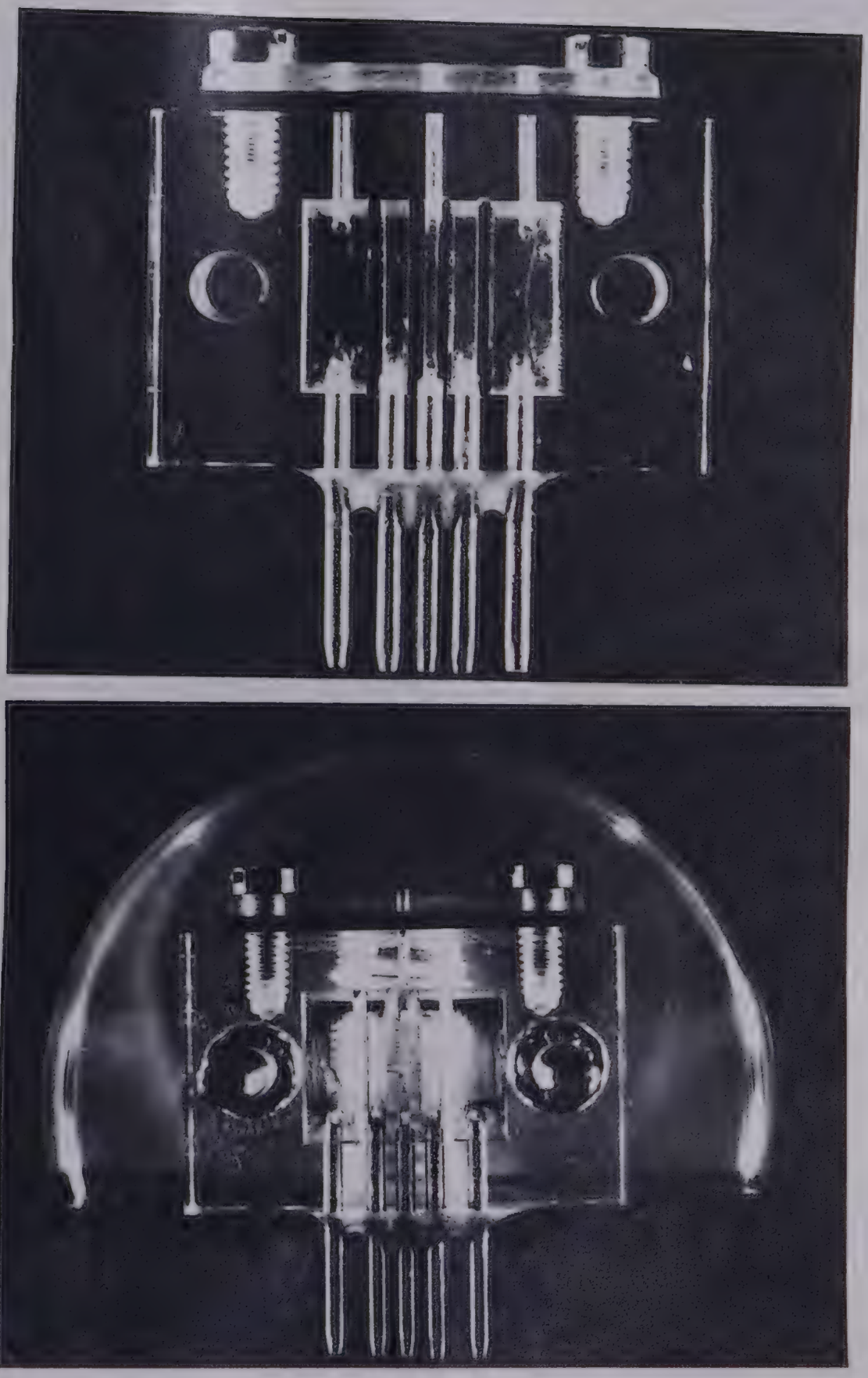

FIGURE 3: Upper (top) and lower (bottom) sections of the perfusion bath. (approximately X 6). Note: (1) Fine groove across partitions of lower section from compartment #1 (left) to compartment #5 (right) (2) Positions of aluminum perfusion tubes, and holes for electrodes (3) Widths of compartments: #1 and #5, 1600µ; #2 and #4, 800µ; #3, 400µ; partition width, 400µ.

microns wide) runs across the centre of each partition in the lower section.

Before the preparation was placed into the groove, the bath was prepared as follows:

(1) Thin, silver-silver chloride electrodes were inserted into holes in compartments 1, 3, and 5 of the upper section and into compartment 3 of the lower section. These electrodes, four in all, were held in place by rubber diaphragms which were clamped to the bath with perspex bars.

(2) To further reduce the chances of fluid communication between compartments, all adjoining surfaces of each section were thinly coated with a nontoxic silicone grease (Valve Seal A; Hopkins and Williams Ltd.). The groove itself was filled with the same grease.

(3) Each compartment in both sections was filled with normal Ringer's solution.

The preparation was manoeuvered into the groove of the lower section of the bath with the help of the attached nylon threads, and the dissecting microscope. This had to be done as rapidly as possible, to avoid evaporation of the Ringer's solution from the muscle surface.

When the preparation was secure in the groove, the top section of the bath was fitted into place over the retaining bolts, and screwed down tightly. The bath was then

mounted on a ringstand inside a Faraday cage, and the perfusion tubes and electrode leads were connected.

The perfusion solutions for each compartment of the bath were stored in two litre flasks which were connected to a vapour trap. All of the storage flasks were arranged on an elevated shelf within the Faraday cage, in an attempt to reduce the amount of 60-cycle pick up by the high resistance leads (see CLAMP STABILITY). Each storage flask was connected to a corresponding aluminum inflow pipe on the lower section of the bath by means of a 3-way stopcock and short length of very thin polyethylene tubing (approximately 0.06 inches in diameter). Individual compartments in the upper section of the bath each contained similar aluminum pipes joined to polyethylene outflow tubes, through which the perfusion solutions escaped into a large collection vessel. The solutions were at room temperature (22°C-23°C), and flowed into the bath under the force of gravity at a rate of 1.5 to 2.0 cc. per minute. The pH of the solutions was approximately 7.2. Vacuum could be established in the collection vessel should a faster perfusion rate be required. Compartments 2 and 4 were perfused with sucrose, compartment 3 with normal Ringer's solution, and compartments 1 and 5 with either normal Ringer's or high potassium-Ringer's solution (see GAP POTENTIAL).

Several times during each experiment, air bubbles entered one or more of the perfusion compartments. If these covered large areas of electrodes or disrupted the sucrose

gap, they could interfere with potential and current recording. Initially, bubbles in the sucrose gap might allow gap jumping (extracellular current flow through the gap) to persist. The bubbles were removed by inserting a fine cannula, which was connected to an empty 5 cc. syringe, into the outflow tube and gently applying a small amount of vacuum.

After each set of experiments, the perfusion baths were cleaned with isopropanol and then rinsed with distilled water. During this series of experiments, several different perfusion baths were used. However, all were constructed from the same design with identical dimensions, and no significant differences in either voltage or current records were noted when the baths were interchanged.

II.5 ELECTRODES:

All potential changes and ionic currents were recorded with silver-silver chloride electrodes. These were prepared in the following way: Short pieces (approximately 3 inches) of fine silver wire (diameter between 0.015 and 0.020 inches) were connected in pairs to the anode of a 1.5 volt battery. A 22 K resistor was connected to the cathode of the battery, and a lead composed of silver wire was soldered to its end. The 22 K series resistor was found by trial and error to sufficiently limit the current density during chloridation so that a mechanically stable chloride coating was produced. The silver leads from the anode and cathode were immersed in an electrolyte solution (10% sodium

chloride) to a depth of approximately 1.5 inches, and chloridation was allowed to proceed for 8 to 12 hours, under dimly lit conditions. After this time, the two leads from the anode were evenly chlorided and ready for use. New electrodes were made for each series of experiments, and no potential fluctuations due to unstable electrodes were observed.

II.6 ELECTRONIC APPARATUS:

Figure 4 is a block diagram of the electronic apparatus that was used to generate rectangular current or voltage pulses, in order to either current or voltage clamp the section of the preparation which was in the centre compartment of the bath.

The membrane potential was indirectly measured (see GAP POTENTIAL) as the potential difference between an electrode in the centre compartment of the bath (which contained normal Ringer's solution) and a second electrode in one of the end compartments. This potential was established after both ends of the preparation had been depolarized by perfusing them with high-potassium Ringer's solution. A differential cathode follower (GRASS P612 with RPS 106 power supply) was used to record this potential difference. The cathode follower had a very high input impedance (10^{11} ohms), low output impedance (10^{3} ohms), and a frequency response which was flat to 60 kilocycles/sec. It therefore was able to produce an unattenuated voltage signal, and drew a negligible amount of current from the preparation. Additional

features of the cathode follower included a variable amplification (X 1 to X 1,000; operated at X 1 in these experiments), and a voltage calibrator, for reference testing of the recorded signals.

From the output of the cathode follower the voltage signal was taken to one of the vertical inputs of a dual beam oscilloscope (Tektronix 502 A). The oscilloscope was equipped with a cathode follower vertical output, and was therefore used as one of the amplifiers in the feedback loop of the voltage clamp circuit.

The membrane currents (those ionic currents necessary to maintain a given potential) were recorded by an electrode in the centre compartment of the bath. These currents were then measured as a potential drop across a small series resistance (1K) to ground, and were displayed on the second beam of the oscilloscope.

Both the membrane potential and ionic currents were recorded on a pen recorder (Beckman RC dynograph, 4 channel), as well as being monitored on the oscilloscope. Although not shown in Figure 4, the pen recorder was connected in parallel with the oscilloscope. The frequency response of the pen recorder (flat to 50 cycles/sec.) was sufficient to allow both the potentials and currents to be accurately recorded, since these experiments were designed to analyse relatively slow current changes (i.e. delayed outward ionic currents, the time constants ranging from 100 msec. to 1.5 sec.). In all experiments, the frequency response of

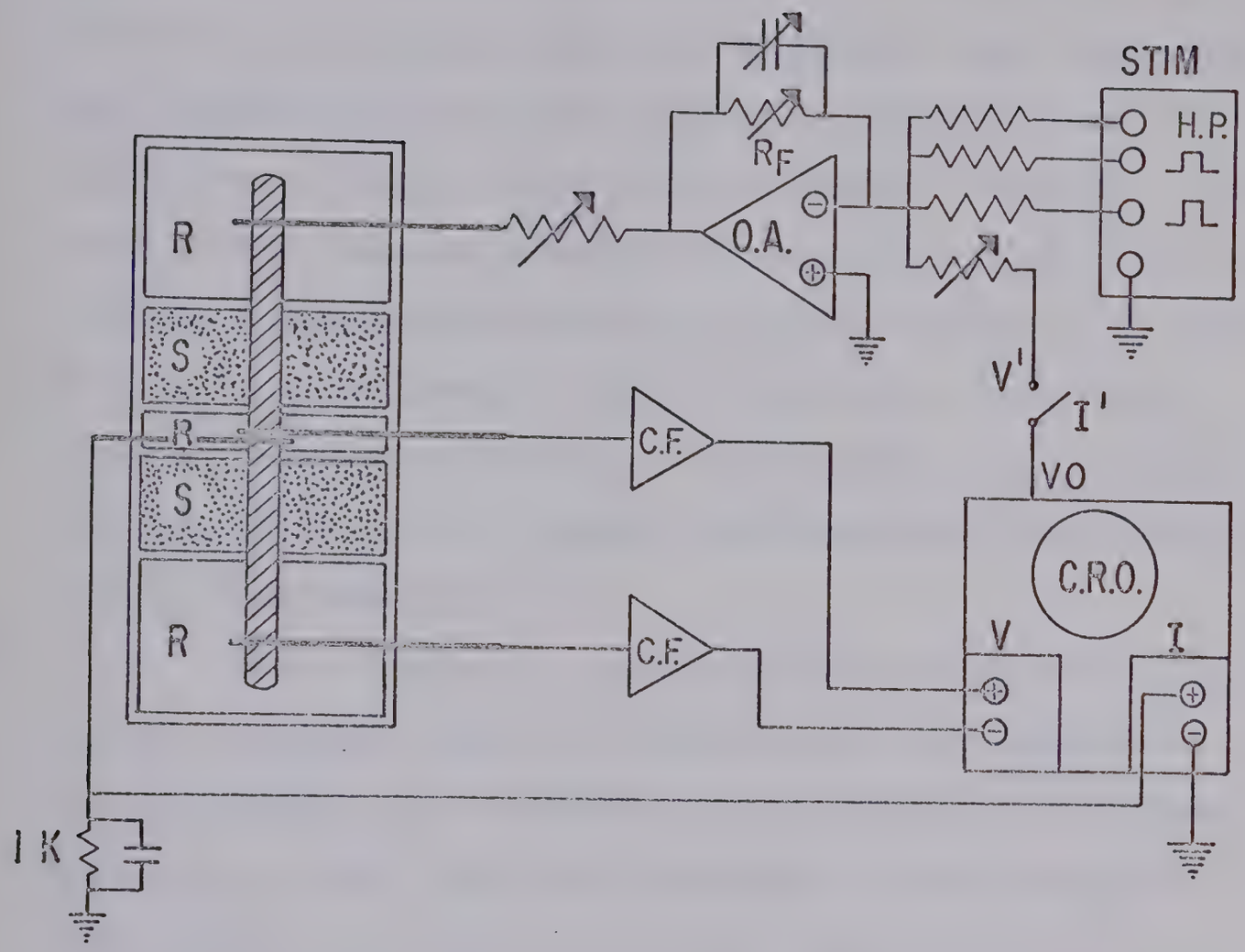

FIGURE 4: Schematic of voltage clamp apparatus. Abbreviations: R. normal Ringer's solution; S. isotonic sucrose solution; CF. cathode follower; CRO. oscilloscope; VO. cathode follower output from oscilloscope. V^1-I^1. switch selecting constant current or voltage clamp mode; OA. negative feedback operational amplifier; R_f. feedback resistor; STIM. stimulator unit; HP. constant d-c potential.

the pen recorder was reduced, but not significantly, by placing an R-C filter (1 K ohm; 1 microfarad) across its input. This filtering was designed to cut down the amount of noise on the current records. Throughout each experiment ionic current changes were recorded at three different amplification levels. In this way, permanent records of the total current changes (onset and decay) during and following a voltage clamp pulse, as well as amplifications of portions of these changes (current tails) could simultaneously be obtained. Amplified records of the decaying ionic currents were essential, for the quantitative analysis of conductance changes (see RESULTS).

The stimulus or command pulses were generated by the unit labelled 'STIM.' in Figure 4 and were applied to the preparation via an electrode in one of the end compartments of the bath. The main components of the stimulator device were: a Devices digitmer (5-figure, Mark II), a low-voltage power supply (H-Lab model 855c), a low-voltage operational amplifier (Motorola MC 1439G), three voltage divider resistance chains, and a high-voltage operational amplifier (Philbrick MLF-100), which was powered by a variable supply (Lambda LP 415 F). This voltage clamp output stage, designed by Dr. D. Noble, was capable of generating rectangular pulses having variable durations, magnitudes, and polarities. These pulses were then used either to pass currents into the preparation, or to provide command pulses for the negative feedback voltage clamp circuit.

Figure 6 illustrates that, in total, three -12 volt supplies were used to generate the two command pulses, and to control the holding potential (see TERMINOLOGY). The two voltage supplies for the command pulses were triggered from the timing pulses of the digitimer; therefore, their durations, cycle period, and magnitudes were variable. However, since the third -12 volt potential was produced by a steady low-voltage power supply within the digitimer, only its magnitude could be varied.

Each -12 volt pulse was initially fed onto the negative summing junction of a low-voltage operational amplifier (Motorola MC 1439G) and then passed across a chain of fixed resistors in series. The function of this part of the output circuit (shown in Figure 5 and labelled 'F' in Figure 6) is two-fold: (1) Since the gain of the operational amplifier is -0.75 (R_F/R_I = 7.5 K ohm/10 K ohm) it allows the polarity of the output pulses to be reversed by the switch labelled 'A'. Note, however, the final output from the MLF-100 will have opposite polarity to that established by the MC 1439G, since the MLF-100 operates in a negative feedback mode. (2) The output from the first stage (± 9 volts) is then connected across a voltage divider resistance chain which allows the output signal to be varied in decade steps up to ± 100 volts in the current mode, or to produce membrane potentials up to ± 200 mV in the voltage clamp mode. The total resistance of the voltage divider circuit, however, has a constant value of 10 K ohms due to

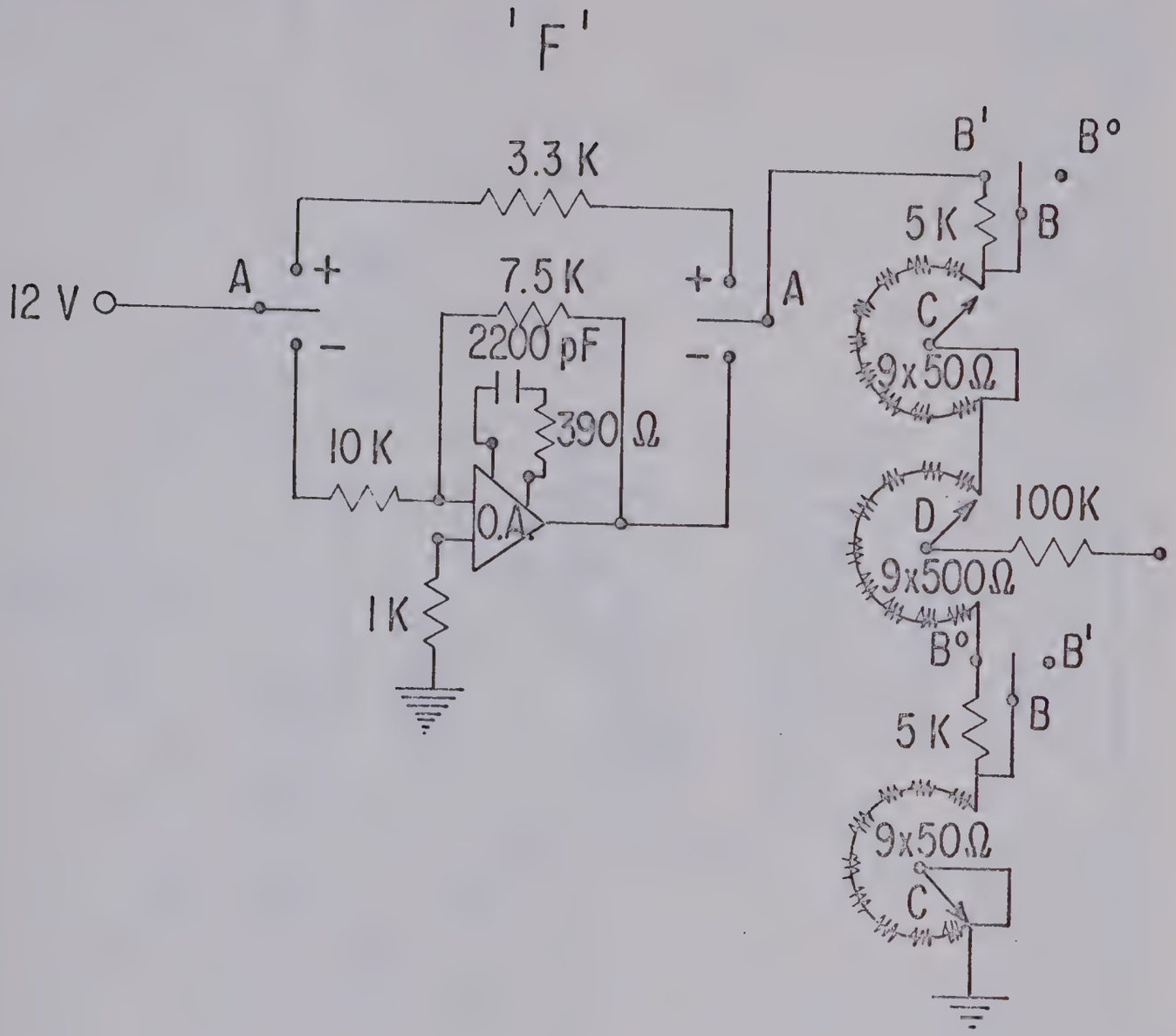

FIGURE 5: Subunit for decade dialling of voltages or currents. The operational amplifier (MC 1439 G) is powered by a low-voltage supply (H-Lab 855C) and operates at a gain of -0.75. When the switches labelled A are in the negative position, the amplifier inverts the -12 volt pulse, and supplies +9 volts to the resistance chain. When the switches labelled A are in the positive position, the amplifier is bypassed, and -9 volts reaches the resistance chain. The ±9 volt input is dialled in steps of 4.5V. (switch B), 0.45V. (switch D) or 0.045V. (switch C). The output pulse from the voltage divider resistance chain is then fed into a second operational amplifier (MLF 100, Figure 6) and is both inverted and amplified. Note that the total resistance of the voltage divider chain is always 10 K, and that the switches labelled A&A, B&B and C&C are ganged.

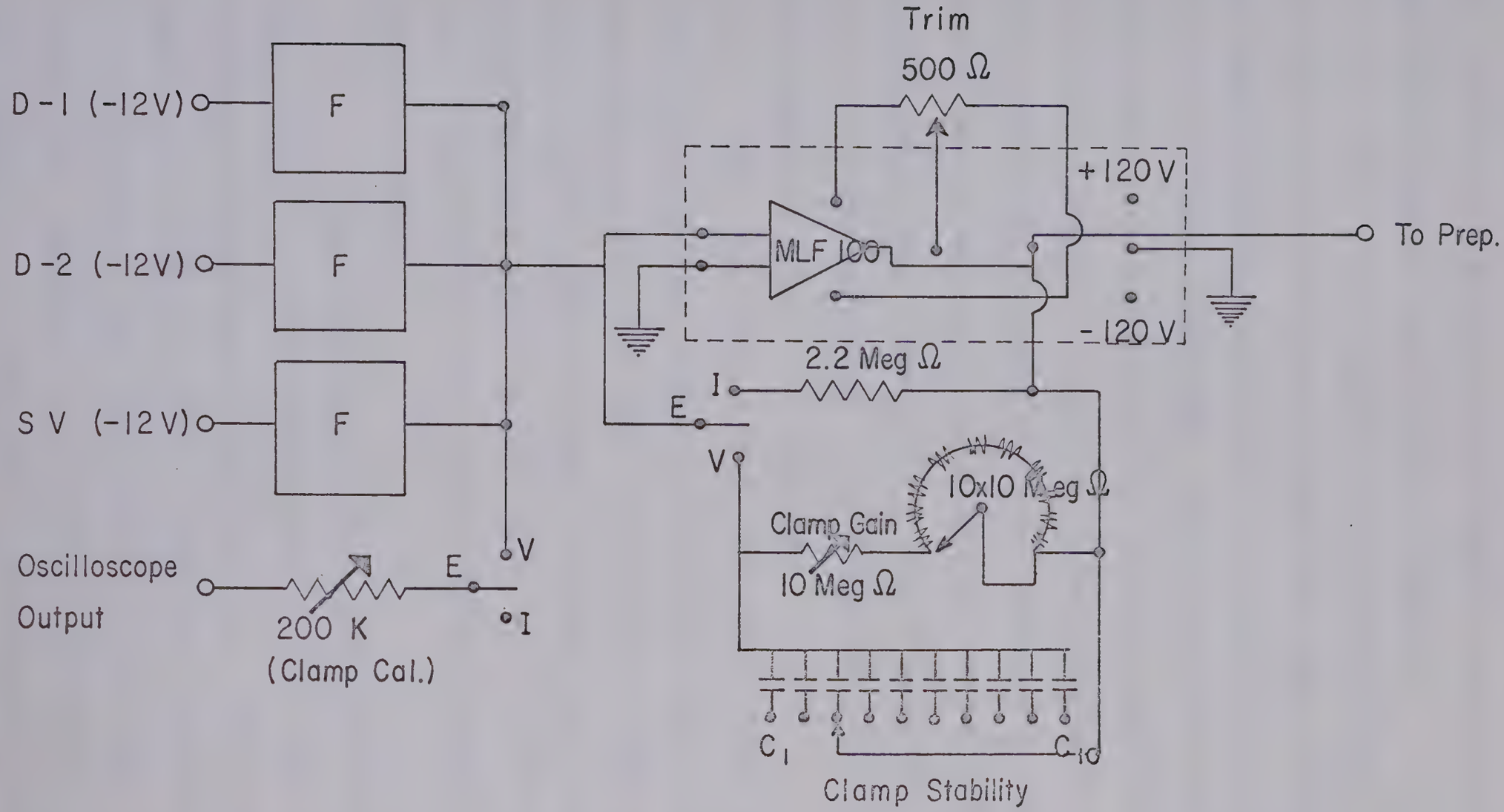

FIGURE 6: Constant current or voltage clamp circuit. When the switch labelled E is in the 'I' position, the voltages fed into the negative feedback amplifier (MLF 100) from the sub-units labelled F (Figure 5) are amplified X 22. This means that the switches B, C and D (Figure 5) dial outputs of 1, 10 and 100 volts with a maximum of about 100 volts. When switch E is in the 'V' position, the voltages produced depend on the setting of Clamp Cal. (see text for details). The switches labelled E are ganged.

the specific arrangement of the switch B, and the fact that the two 450 ohm resistor chains are ganged.

From the voltage divider resistance chain, the voltage pulse was fed across a 100 K ohm input resistor to the negative summing junction of the high-voltage operational amplifier (Philbrick MLF-100). When connected to an appropriate power supply, the MLF-100 was capable of supplying a ± 100 volt output at a current rating of 10 milliamps. The power supply that was used to drive the MLF-100 was a variable high-voltage LAMBDA model (LP-415F), set at 240 volts with positive and negative terminals connected to ground through 2 volt, 27 K ohm resistors. Its output was ± 120 volts with respect to ground, as required.

When the circuit is in the current mode (see Figure 5) the MLF-100 simply reverses the sign of the voltage input and amplifies the input by a constant factor of -22 (R_F/R_I = 2.2 Meg. ohms/10 K ohm). Voltage drops across the resistance chain are therefore amplified to produce decade output steps of 0.99 volts, or 9.9 volts, as well as a single step of 99 volts.

In the voltage clamp mode, the cathode follower output from the oscilloscope is used to feed back an indirect measurement of the membrane voltage (V_m). This is then summed at the negative summing junction of the MLF-100 with the stimulus pulse (V_s) from the resistance chain. On this setting, the magnitude of the voltage pulse that is produced depends on the magnitude of the variable (200 K ohm)

input resistance denoted 'CLAMP CALIBRATION'. The gain of the MLF-100 is determined by a variable feedback resistance composed of a 10 Meg. ohm potentiometer (CLAMP GAIN) connected in series with a wafer containing nine additional 10 Meg. ohm fixed resistances. The frequency response of the clamp circuit was varied by changing the values of the capacitance (variable from 10 pF. to 5,000 pF.) that was in parallel with the feedback resistance.

II.6 (a) VOLTAGE CLAMP CIRCUIT:

These experiments were designed to analyse ionic current flow in response to controlled changes in membrane potential. It is important, therefore, to understand how the circuitry shown in Figure 6 can, in fact, force the membrane potential to follow the command potentials which are generated by the stimulator unit. Figure 7 is a block diagram in which various components of the preparation and the perfusion bath are represented by simplified electronic equivalents.

As was previously mentioned, the membrane potential (V_m) is recorded by a pair of external electrodes and is then fed through a cathode follower to an oscilloscope. The cathode follower output from the oscilloscope (V_o) is therefore proportional to V_m. This potential, V_o, is added to the command potential, V_s, (composed of a steady, d-c potential upon which either one or two independent voltage pulses are superimposed by the digitimer) at the negative summing junction of a high gain operational amplifier (MLF-100).

Since this amplifier is operated in a negative feedback mode, it both amplifies and reverses the sign of the input $(V_o + V_s)$, giving an output of $-A(V_o + V_s)$, where A is the amplification factor of the MLF-100. This output voltage is then applied to an external electrode in one of the end compartments of the bath. Because of the high resistivity of the sucrose gap (R_{s_1} and R_{s_2}) virtually all of the current (which is produced by the applied potential), flows intracellularly from the end compartment to the centre compartment, where it is collected and recorded as a potential drop across a small resistance (R_G) to ground.

It can easily be shown that, provided A is sufficiently large, the current flow resulting from the MLF-100 output voltage, will force V_o to follow $-V_s$ very closely.

1. If V_o is greater than V_s, in effect, a hyperpolarizing command pulse has been applied. In this case, the amplifier output, $-A(V_o + V_s)$, will be large and negative, and an inward hyperpolarizing current will flow across the membrane in the test compartment, causing V_o to hyperpolarize towards $-V_s$.
2. However, if V_o is smaller than V_s, the depolarizing command pulse causes a positive voltage output from the MLF-100, and produces an outward depolarizing current flow across the clamped membrane. This causes V_o to depolarize towards $-V_s$.

Note that the amplification factor, -A, must be very large if V_o is to accurately follow $-V_s$. 'A' is controlled by the gain of the MLF-100 amplifier, which in the feedback mode is given by the following quotient: R_F/R_I. The amplifier gain, therefore, may be varied by changing R_F (see Clamp Gain, Figure 6). The variable capacitance which is in parallel with the feedback resistance, regulates the frequency response of the amplifier output (see CLAMP STABILITY).

At the summing junction of the MLF-100, the currents produced by the voltages V_o and V_s are added; not the voltages themselves. The exact magnitude of these currents will be given by V_o/R^O_{IN} and V_s/R^I_{IN}. The fact that the current flow is proportional to the input resistance values suggests a simple method of calibrating the output from the MLF-100 in terms of the decade dialling which is available from the stimulator unit. One simply varies R^O_{IN} (a 200 K potentiometer) until the actual clamp pulse magnitude corresponds to the dialled magnitude, which is selected on the decade dialling system. When this is the case, the current flowing into the amplifier as a result of dialling, for example, a 10 mV pulse must be equal and opposite to the current produced by a 10 mV change in membrane potential.

In the constant current mode, the cathode follower output from the oscilloscope is disconnected. Therefore, the input to the MLF-100 is V_s. The corresponding voltage

output, $-A(V_s)$, then passes constant current pulses into the test compartment of the bath.

II.6 (b) CLAMP STABILITY:

In principle, using the double sucrose gap technique to control membrane potentials is quite straightforward. In practice, however, it can be rather difficult. Difficulties may arise from either the physiological state or anatomical features of the preparation (see CLAMP UNIFORMITY); however, technical problems resulting from instability of the feedback circuit are also frequently encountered. This instability causes high frequency oscillations of both the command potential and the resulting membrane currents. Therefore, it destroys the preparation for quantitative analysis.

The basic requirements for stability in a voltage clamp, negative feedback circuit (Figure 7) are the following: (1) A phase angle of 180 degrees between the output and the input of the feedback amplifier must be maintained. A shift in this phase angle alters the relation between the magnitude of the negative feedback potential (output potential) and the command potential (input potential). If the phase shift is great enough the membrane potential can no longer approach the command potential and the circuit becomes unstable. (2) Secondly, the entire output from the negative feedback amplifier must be applied to the part of the preparation that is to be uniformly polarized. If

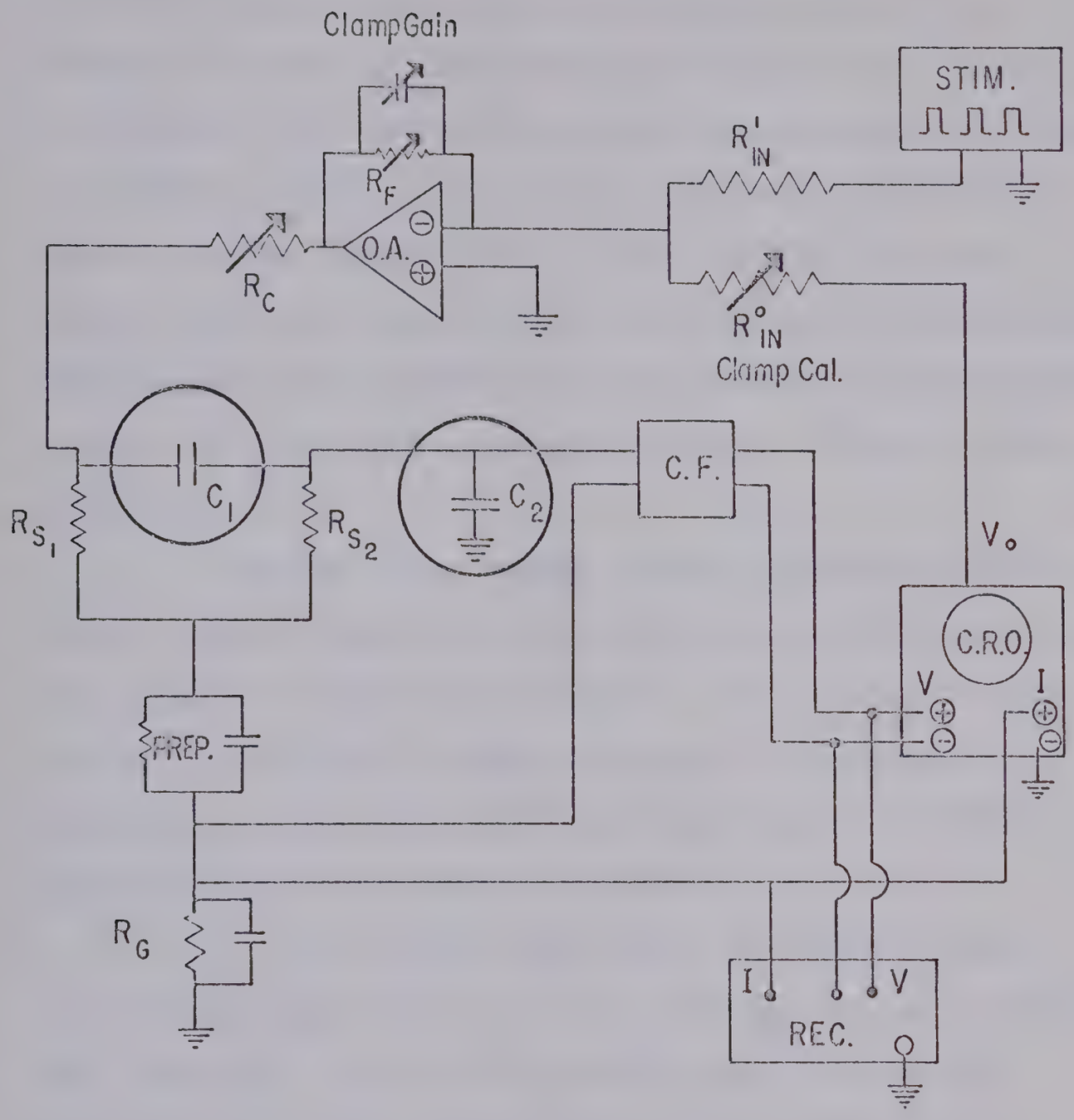

FIGURE 7: Schematic of voltage clamp circuit. C_1 and C_2 (circled) are sources of capacitative coupling which give rise to clamp instability. The preparation (PREP.) and perfusion bath (R_{S_1} and R_{S_2}) are represented by simplified electronic equivalents. Abbreviations: CRO. oscilloscope; VO. cathode follower output from oscilloscope; STIM. stimulator; R^0_{IN}, R^1_{IN} input resistances; OA. operational amplifier (MLF 100); R_F feedback resistance; R_c variable resistance; R_{S_1} and R_{S_2} resistances of sucrose gaps; R_G resistance to ground monitoring current flow; REC. pen recorder.

alternate pathways for current flow through the voltage recording system exist, then the recorded difference between the membrane and command potentials will include an artifact. The feedback amplifier then attempts to force the membrane potential to follow this 'error potential' and may initiate oscillation. The condition that the entire amplifier output must be applied to the preparation implies that any alternate current pathways, such as shunts around high resistances, may be capable of causing clamp instability.

The two major causes of high frequency oscillations in these experiments were the stray capacitances C_1 and C_2 that are shown in Figure 7. Both of these capacitances do, in fact, provide alternate low impedance pathways, through which the high frequency components of applied currents may flow to ground.

In the voltage clamp mode, the sucrose gaps provide two high resistances, R_{S_1} and R_{S_2}, (approximately 50 Meg. ohm each) across which current must flow within the perfusion bath. For example, the resistance R_{S_1} forces applied current to flow intracellularly through the gap before it can reach the centre compartment, where it flows to ground across R_G. The voltage is also recorded across a high resistance, R_{S_2}.

The stray capacitance, C_1, introduces capacitative coupling between two leads which are separated by the high

resistances of the sucrose gaps. High frequency components of the amplifier current may therefore bypass R_{S_1} and flow to ground through this (C_1) low impedance pathway. In doing so, they may pass through the opposite sucrose gap, R_{S_2}, and then to ground across R_G. This kind of capacitative coupling could result from (i) insufficient shielding of these 'high resistance' leads, allowing the voltage recording lead to pick up high frequency currents from the lead connected to the amplifier output; or (ii) from an increased resistance in the S_1 sucrose gap, which is frequently due to the presence of air bubbles. This increased resistance would make it more difficult for current to flow through the normal pathway, and easier for it to flow across C_1.

Capacitative current from C_1 can also completely bypass the preparation by flowing through C_2 to ground. C_2 represents a stray capacitance resulting from excess shielding of the voltage lead. This pathway for current flow would be preferential, if for example, R_{S_2} was very high.

Clearly, if there is an appreciable current flowing through either C_1 or C_2 the conditions for stability in the feedback loop will not be satisfied. In fact, the feedback loop in Figure 7 was most stable when (i) the amount of shielding that was necessary was reduced to a minimum by placing the cathode follower probe very close to the preparation; and (ii) very short leads, placed as far away from each other as possible, were

used to apply current and to record membrane potential.

The high frequency components that are superimposed on the command pulses can be reduced by adding various compensating devices to the feedback circuit. Since it is only the high frequency currents which charge the stray capacitances, reducing these currents should correspondingly decrease the effect of capacitative coupling between the 'high resistance' leads, and therefore increase the stability of the voltage clamp. The amount of compensation that is possible, however, is limited because the compensating devices may significantly prolong the rise time of the clamp pulse (about 3 msec. in our system).

One compensating device involves placing a small variable capacitance in parallel with the feedback resistance. This reduces the gain of the feedback amplifier at high frequencies. The variable capacitance across R_f (Figure 7) has a range of 10 picofarads to 5000 picofarads, and is commonly set at 250 picofarads.

A second device which reduces the amount of high frequency component in the output current is the variable resistance, R_C, which is situated at the output point of the feedback amplifier. R_C is set at 10 Meg. ohm in the constant current mode, and at 2.0 Meg. ohm in the voltage clamp mode. This resistance is in series with the stray capacitances, C_1 and C_2, and thus increases the impedance of the alternate pathways for high frequency current flow.

In some preparations, low frequency oscillations occurred when the command potential polarized the preparation into the threshold region for activation of the rapid inward sodium current (approximately -50 to -60 mV). Since the activation of I_{Na} is extremely rapid (probably less than 2 msec.) and its magnitude is very large, these oscillations could have resulted from phase lag within the feedback loop, or from limitations of MLF-100 output. A more probable explanation, however, is that the oscillations were produced by non-uniformly polarized regions within the test compartment. Since the sodium spike corresponds to an approximately one hundred-fold increase in sodium conductance (Weidman, 1951), then the space constant of the preparation, would be reduced to about 10 per cent of its value in the resting state. If this was the case, the gap width (400 microns) should greatly exceed the magnitude of space constant, (see CLAMP UNIFORMITY). Marked voltage decrements in the test region would then result. The low frequency oscillations of voltage and currents, therefore, may have been produced by regions of the preparation which had escaped from the command potential. Beeler and Reuter (1970a), in their attempts to quantitatively study the inward currents in canine papillary muscle, have observed non-uniformity in the region of the sodium threshold. However, they attribute it mainly to the anatomical features of the preparation, which produce a resistance in series with the membrane capacitance.

II.6 (c) CLAMP UNIFORMITY:

The ionic currents which maintain a given membrane potential are both time-and voltage-dependent. Hence, before these currents can be quantitatively analysed, the entire region of the preparation from which they are recorded must be uniformly polarized to some known potential. In any passive cable-like structure, an applied current rapidly decreases with increasing distance. Therefore, the length of the preparation that is to be voltage clamped must be small compared to the space constant of the preparation.

Unfortunately, the space constant for frog atrial muscle has not been accurately determined. Trautwein, Kuffler and Edwards (1956) give values which range from 230 microns to 410 microns. Since atrial trabeculae almost certainly are not simple one-dimensional structures, part of the observed variability may result from either two-dimensional, or three-dimensional spread of the applied current.

The width of the centre compartment of all perfusion baths used in these experiments was 400 microns. However, the length of the preparation actually exposed to the applied clamp currents was less than this, because the silicone grease inevitably spread into the centre gap when the two sections of the bath were brought together. The effective width of the gap was estimated to be 300 microns. Therefore, the region of atrial muscle that was voltage

clamped probably varied between 0.5 and 1.0 space constant.

The condition that all of the intracellular current must leave the cells within the centre compartment requires the test portion of the preparation to be treated as an open-circuited short cable (Weidmann, 1952; Adrian and Freygang, 1962). Assuming that this cable is linear, lengths between 0.5 and 1.0 space constant would be subject to voltage decrements of 10 and 30 per cent respectively.

Several independent lines of evidence, however, suggest that the space constant of frog atrial muscle is substantially larger than 400 microns. Anatomical studies by Barr, Dewey, and Berger (1965), and Baldwin (1968) have shown many lateral connections between atrial cells. Current spread from a small current source, therefore, is probably not limited to one dimension. If multi-dimensional spread occurs, then the amount of voltage decrement for a given distance is markedly increased (Noble, 1962). Since this rate of decrement is used to calculate the space constant, Trautwein et al, assuming simple one dimensional geometry, may have substantially underestimated the space constant.

Brown and Noble (1969a) have performed experiments using perfusion baths whose test compartments varied between 200 and 500 microns in width. Within this range, no significant differences in delayed current responses were observed. This would indicate that the magnitude of the space constant is nearer to 500 microns than to 200 microns.

Haas, Kern and Einwachter (1970) directly tested the spatial uniformity of an applied potential across a 200 micron centre gap by using an intracellular microelectrode to measure the membrane potential at various distances from the current source. Although their method was sensitive to potential changes as small as 2 mV, no steady state variation of potential with distance was recorded. Assuming that these records were obtained from cells at the surface of the preparation, no radial decrements could be involved. Therefore, the space constant for atrial muscle may easily be as large as 1.0 millimetre.

It seems likely, then, that the axial decrement of the command potential, which is determined by the space constant, is negligible within a 400 micron test gap. However, since, the preparation has a diameter of approximately 300 microns, the possibility of radial voltage decrement must be considered.

The tight packing of the fibre bundles in the trabeculae and the narrow clefts between cells where there are no cardiac adhesion plaques or close junctions (Baldwin, 1968), could present a high resistance to radial current flow. Beeler and Reuter (1970a) have shown that in canine papillary muscle this 'cleft' resistance is in series with the membrane resistance of the fibres. Therefore, when the membrane currents are large (for example, during the sodium transient), the potential drop across the 'cleft' resistance becomes appreciable. Since the 'cleft' potential is in series with the membrane potential, the voltage clamp

apparatus forces the sum of these two potentials, rather than the membrane potential only, to follow the command potential. However, in these experiments, only the smaller, delayed outward currents were analysed; therefore, this kind of artifact may not be a problem.

II.7 ELECTROPHYSIOLOGY:

(a) GAP POTENTIAL:

At the start of an experiment, compartments 1, 3, and 5 of the bath were perfused with normal Ringer's solution. Once the action potential no longer propagated through the sucrose chambers (the external resistance in the sucrose gap had reached a sufficient magnitude to prevent extracellular current flow) the solutions perfusing compartments 1 and 5 were changed to high-potassium Ringer's solution.

This change caused a negative going base-line shift (Figure 8). Provided that the resistance to extracellular current flow in the sucrose gaps is great enough, this 'gap potential' is theoretically equal to the average resting potential of the fibres in the preparation.

The values of the gap potential that were recorded in these experiments ranged between 65 and 95 mV. and were associated with action potentials ranging between 90 and 130 mV.

These gap potentials appear to agree well with values of resting potentials that have been recorded intracellularly from atrial muscle. Glitsch, Haas and Trautwein

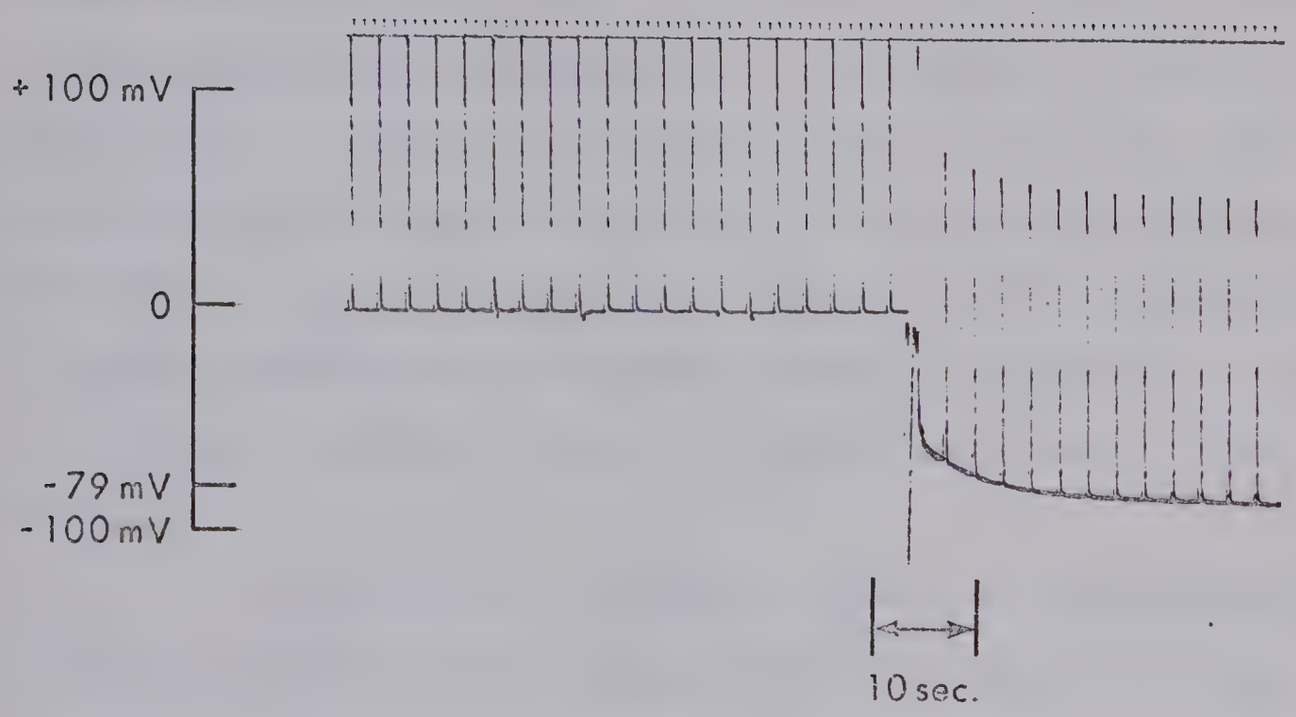

FIGURE 8: Voltage record during change of fluid perfusing outer compartments of the bath from normal Ringer's (2 mM K^+) to high-potassium Ringer's (112 mM K^+). The negative baseline shift (the gap potential) approximates the resting potential of the preparation. The initial baseline corresponds with the zero on the voltage calibration, therefore the magnitude of this gap potential is about -79 mV.

(1965) recorded resting potentials of -75 ± 4.6 mV and action potentials of 89 ± 0.2 mV from frog atrium. Haas, Kern, and Einwachter (1970), also studying the frog atrium, directly recorded resting potentials of -72 ± 4.0 mV.

Therefore, in these experiments, gap potential measurements have been used as a guide to the general state of the preparation and apparatus. For example, a preparation giving a large action potential but only a small gap potential would suggest some fault in either the electrical recording or perfusion systems. When these two values are in good correspondence, the gap potential appears to provide an accurate estimate of the true resting potential of the fibres.

In addition to providing a means of estimating the resting potential of the preparation, the change to high-potassium Ringer's solution in compartments 1 and 5 offers a further advantage. Current should, under these conditions, enter the preparation more easily since the conductance is usually substantially increased when the membrane is depolarized. This should, in turn, reduce the proportion of current flowing externally and therefore increase the effectiveness of the voltage clamp.

II.7 (b) TERMINOLOGY:

(cf. Brown and Noble, 1969a)

Resting Potential: Direct, intracellular recordings of atrial muscle fibre resting potentials were

not done in these experiments. However, the recorded gap potentials are sufficiently similar to resting potential values reported by Haas, Kern and Einwachter (1970) to be considered an accurate estimate of the actual resting potential.

Holding Potential: This is the potential, measured as a deviation (mV.) from zero potential, to which the preparation is clamped for a considerable period of time. The holding potential is maintained by the steady d-c potential of the -12V digitimer supply and can be adjusted by decade dialling in the appropriate voltage divider circuit. Variable duration depolarizing or hyperpolarizing command pulses are superimposed on the holding potential.

Deactivation: This term refers to the switching off of a current by a potential change which is in the opposite direction to that which switches it on. Deactivation, therefore, is the reverse of activation.

Inactivation: This refers to the switching off of a current at the same potential level at which it was switched on. Hence, inactivation is not the opposite of activation, rather, it is an additional process.

III. RESULTS:

In this study, two different kinds of electrophysiological experiments were done. Initially, the responses of the preparation to constant depolarizing current pulses of different durations and magnitudes were recorded.

Secondly, various kinds of voltage clamp experiments were performed. These were designed to analyse the outward components of the membrane currents which underlie the potential changes occurring during the action and pacemaker potentials.

III.1 CONSTANT CURRENT EXPERIMENTS:

Virtually all of the muscle strips that were dissected from the atria were naturally quiescent. However, both action potentials and pacemaker activity could frequently be induced by low magnitude, depolarizing current pulses.

In particular, small (0.25 μA to 0.50 μA) depolarizing current pulses of very short durations (20 msec.) were nearly always capable of initiating an action potential. The atrial action potentials recorded in these experiments were usually triangular in shape, and were characterized by (i) a rapid depolarization, and (ii) an extremely short plateau region, followed by (iii) an almost linear repolarization to the resting potential. It is worth noting that neither an initial, rapid repolarization phase nor a diastolic depolarization are present in the

normal atrial action potential. Figure 9A illustrates a range of shapes, magnitudes, and durations of action potentials that were recorded during these experiments.

The magnitude and the duration of the action potentials varied between 110 - 130 mV and 400 - 600 milliseconds, respectively. Since the resting potential, as measured by the gap potential, was approximately 80 - 90 mV, the overshoot of the action potentials must have been between 40 - 50 mV.

The size and shape of the action potentials were used as criteria for judging the physiological condition of the preparation, and for detecting the presence of significant leak currents. In general, if (i) the initial magnitude of the action potential was less than 100 mV or (ii) if within a test period (approximately twenty minutes during which action potentials were induced at a frequency of 20 per minute) the magnitude decreased, or its shape changed significantly, then the preparation was discarded.

Healthy preparations giving a consistent, predictable response, were then depolarized at both ends with high-potassium Ringer's solution. Any resultant changes in the appearance of the action potential were considered to indicate the presence of leak current flowing through the sucrose gaps. A significant amount of leak current usually caused the repolarization phase of the action potential to assume a more concave shape, or its magnitude and duration to change. However, since the rate of

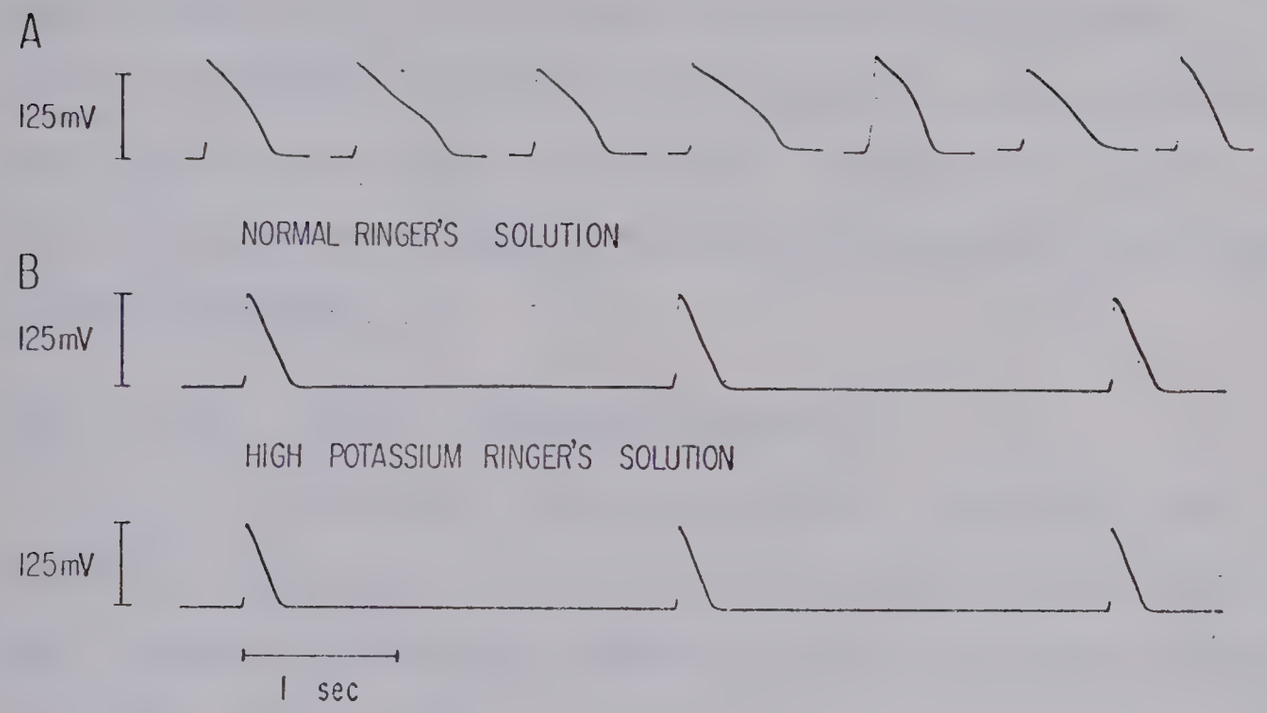

FIGURE 9: PART A. A series of atrial action potentials, each recorded from a different experiment. Note the variation of shape, magnitude and duration. PART B. Comparison of action potentials from the same preparation in which the end chambers of the bath are perfused (i) with normal Ringer's solution and (ii) with high-potassium Ringer's solution. Note the slightly reduced magnitude and duration, but negligible change of shape of the action potential when the ends of the preparation are depolarized.

repolarization in atrial muscle is very small, the net outward current must also be small. Hence a small amount of leak current may cause considerable changes in the potential level and the time course of the action potential. In the example chosen for Figure 9B, therefore, although both the duration and magnitude of the action potential have changed after depolarization, the leak current is almost certainly small enough to allow reliable voltage clamp analysis. The most probable origin of leak current in our experiments was faulty grease seals between the compartments in the bath, allowing the Ringer's solution to mix with the adjacent sucrose solution.

III.1 (a) INDUCED PACEMAKER ACTIVITY:

Relatively long duration (5 - 10 sec.), low magnitude (0.10 μA - 0.60 μA) depolarizing current pulses were capable of inducing pacemaker activity in most preparations (see Figure 10). In every case, there were upper and lower voltage thresholds, above and below which pacing could not be induced. Within this activation range, the frequency of the pacemaker activity depended upon the level of potential generated by the current stimulus.

The maximum pacing frequency in the example chosen for Figure 10 occurred when the preparation was depolarized to approximately -50 mV. This closely corresponds to the optimal potential reported by Brown and Noble (1969a) as being applicable for preparations taken from Rana ridibunda.

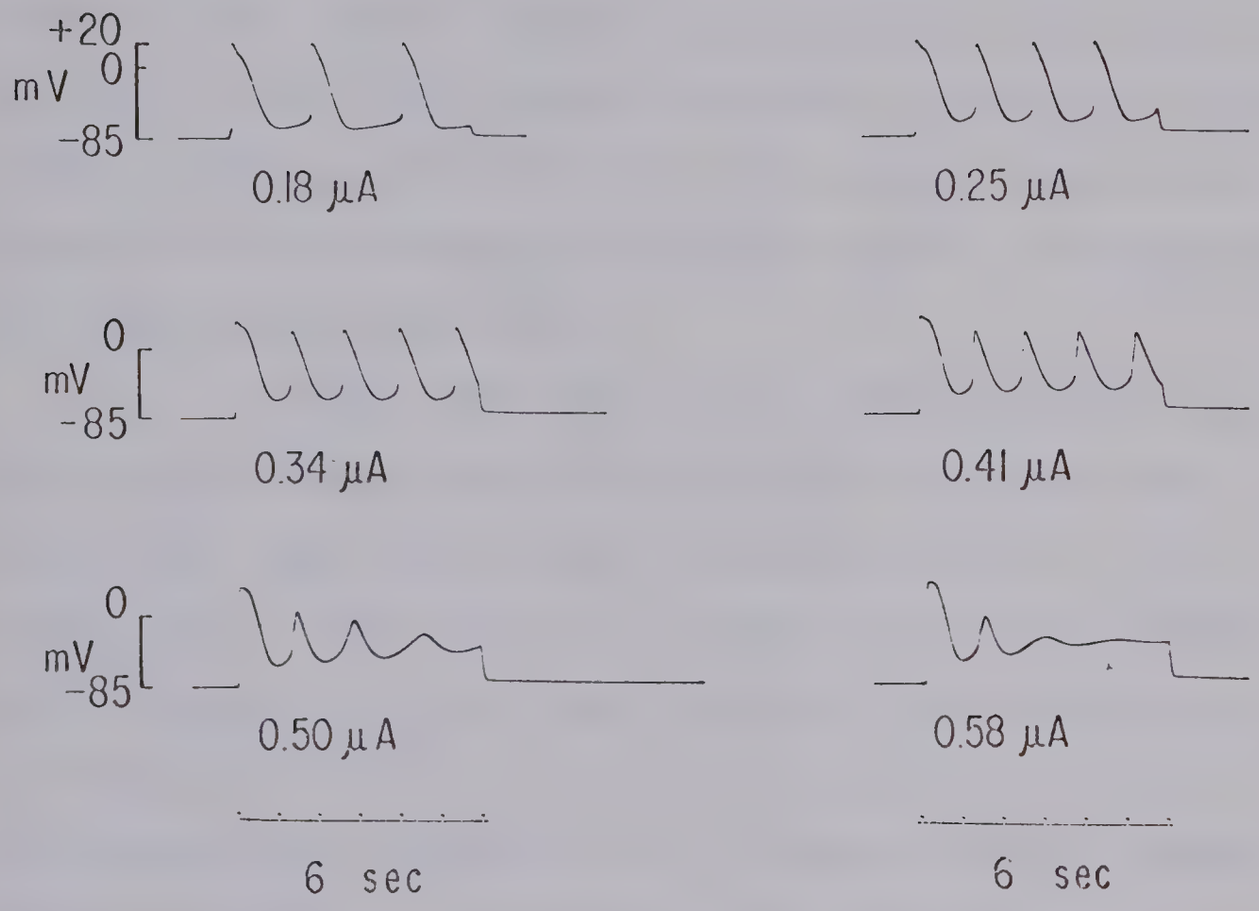

FIGURE 10: Responses of an atrial muscle strip to long duration (6 sec.), low magnitude, depolarizing current pulses. The repetitive responses, or pacemaker activity, reach a maximum frequency when the preparation is depolarized to about the -50 mV level. The current inducing each voltage response is given below the corresponding record.

Certain features of this induced pacemaker activity closely resemble spontaneous pacemaker responses. For example, for relatively small (0.18 μA - 0.41 μA) values of depolarizing current stimuli, the responses of Figure 10 bear a resemblance to natural pacemaker activity in the sinus region (Toda, 1968). However, larger depolarizations produce a response which more closely resembles a damped oscillation than a cardiac pacemaker. It is of interest therefore to compare induced pacemaker activity to models for mechanical and electrical oscillators.

A second important feature illustrated in Figure 10 is the long lasting depolarization which occurred when relatively large depolarizing currents (0.50 μA - 0.58 μA) were used to induce pacing. Although this effect cannot easily be seen at these magnifications, close inspection of Figure 10 shows that, following the 0.50 μA stimulus, the preparation remained slightly depolarized for approximately 4 seconds. This phenomenon was very frequently observed after strong depolarizations. One possible explanation is that it represents the decay of an accumulation of positive ions in the restricted extracellular spaces of the muscle strip.

III.2 (b) SPONTANEOUS PACEMAKER ACTIVITY:

One of the preparations exhibited spontaneous pacemaker activity (see Figure 11). The pacing however, was abolished immediately after the ends of the strip were

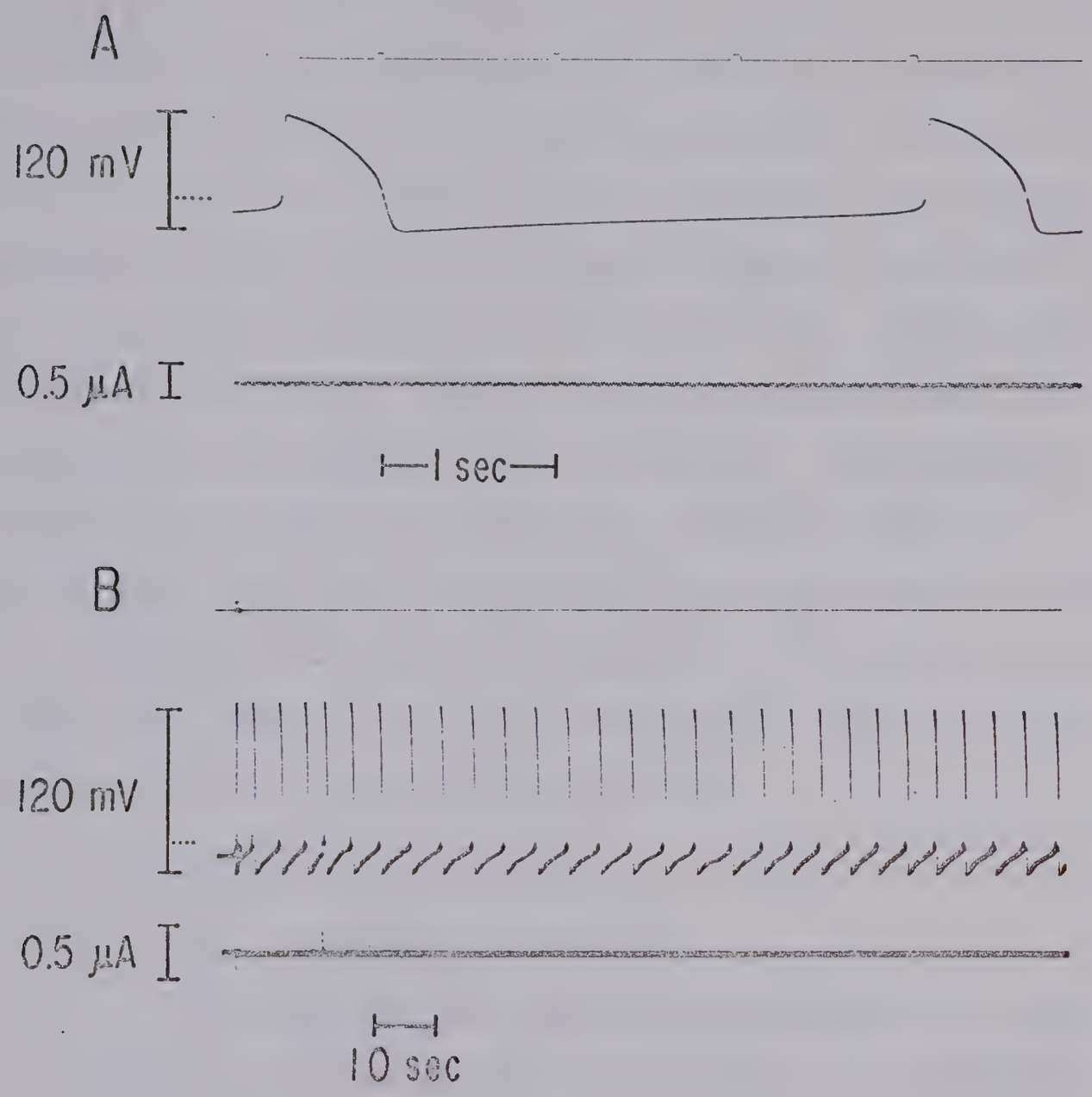

FIGURE 11: Record of a spontaneously active preparation. PART A, recorded at a high paper speed, shows the action potential shape, the natural pacing frequency, and the development of the diastolic depolarization or pacemaker potential. PART B, recorded on a much slower speed, is a second record of spontaneous pacing from the same preparation. The broken line on the voltage calibration indicates the magnitude of the pacemaker potential (approximately 30 mV).

depolarized with high-potassium Ringer's solution. Therefore, an accurate estimate of the resting potential could not be obtained, but the action potential magnitude was approximately 120 mV and the corresponding pacemaker depolarizations were about 30 mV. Typical action potentials and pacemaker potential values from sinus tissues, however, are about 50 to 60 mV and 15 to 20 mV, respectively (Toda, 1968; Hutter and Trautwein, 1956). Hence, this activity may have been generated by an ectopic atrial pacemaker. The pacemaker region of the strip must have been located in the end compartment from which the voltage was being recorded since (i) originally (not shown in Figure 11) the action potential record was inverted, and (ii) depolarizing the end compartments terminated the spontaneous pacing.

III.2 VOLTAGE CLAMP ANALYSIS:

(a) ACTIVATION THRESHOLD:

To establish the range of potentials over which the membrane currents in each preparation were activated, the following experiment was performed. The holding potential was initially set equal to the resting potential (as determined by the gap potential), and was then progressively increased in a series of 10 mV steps. Figure 12 illustrates that in one preparation very little outward current was activated at potentials more negative than -50 mV. At more positive potentials, however, each step depolarization of the holding potential produced (i) an instantaneous, and

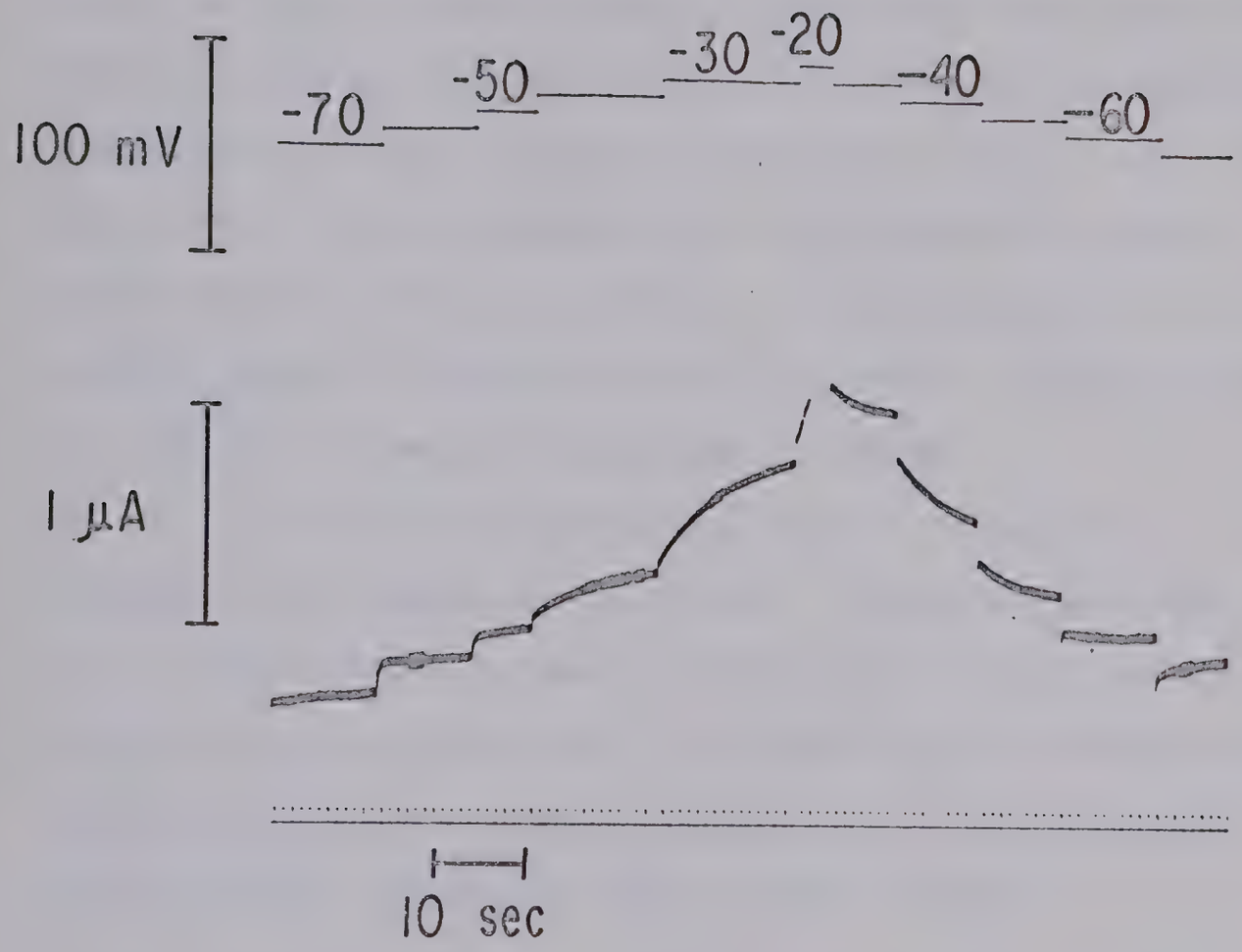

FIGURE 12: Voltage clamp record showing a sequence of 10 mV step changes in membrane potential (upper trace) and the accompanying current changes (lower trace). In this, and each following Figure, an upward deflection of the current trace from the baseline corresponds to an outward current. Note that depolarizations activate only very little outward current until the apparent threshold (approximately -40 mV) is reached. Hyperpolarizing potential changes deactivate the outward currents in a corresponding fashion.

(ii) a time-dependent activation of outward current. Corresponding hyperpolarizing steps of the holding potential produced similar patterns of current deactivation.

In this experiment, the duration of each step change of potential was insufficient to allow a steady state current to be reached, therefore the total magnitude of current activated at each potential could not be determined. In addition, since only 10 mV potential changes were used, the exact voltage threshold for activation of outward current could not be determined. Nevertheless, it is evident that the outward current becomes a steep function of membrane potential beyond about -30 mV.

The holding potential for the subsequent analysis therefore was chosen to be -30 mV. From this holding potential, depolarizing pulses rapidly activate a significant amount of outward current. The decay tails produced by the deactivation of the outward current can then be used to determine the kinetics of the current changes.

III.2 (b) VOLTAGE-DEPENDENCE OF OUTWARD CURRENTS:

From Figure 12 it is clear that, in the frog atrium, the activation and deactivation of the outward membrane currents are both time- and voltage-dependent. Hence, in order to study the voltage-dependence of the membrane currents it is necessary to eliminate the time-dependence. This may be done by applying sufficiently long duration depolarizations, to allow the resulting current changes to reach steady-state levels.

Unfortunately, steady-state analysis is virtually impossible in atrial muscle from Rana catesbeiana. In these preparations, relatively large, long duration depolarizations produce large outward currents. This current flow may cause concentration changes in the restricted extracellular spaces, and may therefore alter the resting membrane potential. The driving forces (eg. E_M-E_K) which generate the membrane currents are then changed. These changes exclude the possibility of performing quantitative studies of the voltage-dependence of the membrane currents, under normal conditions.

Figure 13 illustrates an experiment in which many of the voltage-dependent properties of the delayed outward currents are shown. In this experiment, a succession of long duration, depolarizing pulses were applied from a holding potential of -50 mV. However, in most cases, the depolarizations were not sufficiently long to allow the current changes to reach steady-state values. Each depolarization from the holding potential gave rise to (i) an immediate current change, and (ii) a slower time-dependent activation of current. When the clamp pulse was terminated, the following changes occurred (i) an immediate decrease (ii) a slower, time-dependent deactivation or 'decay tail'.

Several important observations may be made from the family of current records in Figure 13. Depolarizations having magnitudes between +10 mV and +50 mV each produce a very small, but almost identical, amount of immediate

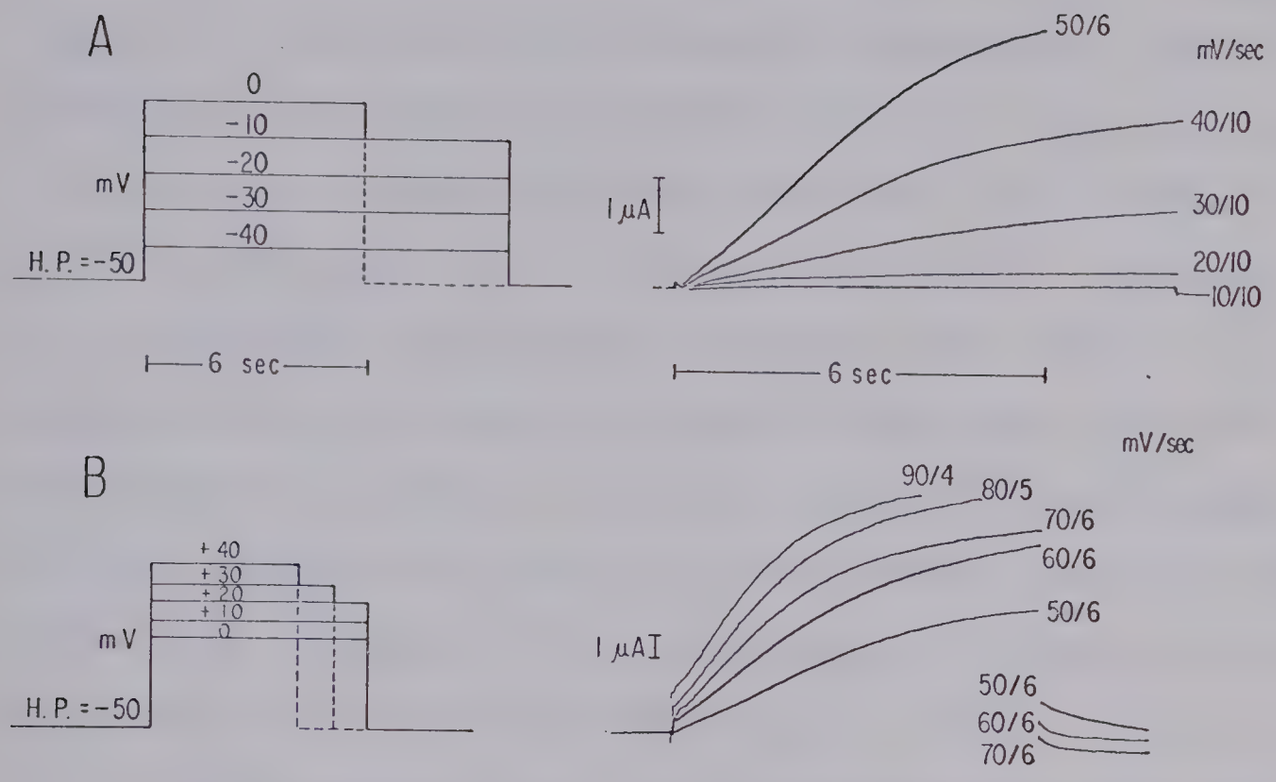

FIGURE 13: Voltage- and time-dependent activation of slow outward currents. Pen recordings of membrane currents are photographically superimposed (right) and the corresponding voltage clamp pulses are drawn (left). Labels on the clamp pulses indicate the absolute level of depolarizations, while labels on the current records indicate the magnitude of the depolarization from the holding potential (ie. 40/10 is a 40 mV depolarization for 10 sec.). NOTE: (i) the gain has been changed between parts A and B, therefore the pulse, 50/6, is shown in duplicate, and (ii) the decay tails for the majority of the pulses are not shown.

(virtually instantaneous) change in outward current. However, all larger depolarizations (+60 mV to +90 mV) produce increased initial outward current changes. Therefore, the 'instantaneous' current-voltage diagram will be virtually flat from the activation threshold (approximately -50 mV) to 0 mV, and will have a positive slope at more depolarized potentials. It is apparent that in response to progressively larger depolarizations, the slower, time-dependent current changes increase in magnitude, and are activated more rapidly. It is not possible to accurately record steady-state levels of current change for depolarizations larger than +20 mV. Nevertheless, it appears that the responses to +80 mV and +90 mV depolarizations approach a very similar maximum value. This suggests that the time-dependent outward current changes become fully activated at approximately +30 mV.

Further information regarding the voltage-dependence of the membrane currents may be obtained by analysing the pattern of current decay that is produced when the clamp pulse is terminated. The decay tails shown in Figure 13B show that the largest depolarization (+70 mV) has produced the smallest decay tail. Conventionally, the amplitude of the decay tail is used to measure the amount of conductance which has been activated by the preceding depolarization (cf. Hodgkin and Huxley, 1952c). This measurement is valid only if (i) the slow current onset is generated entirely by the conductance component(s)

which underlie the decay, and (ii) the driving force remains constant. The magnitude of the decay is then a function of the duration and level of the preceding depolarization; and the time constant of decay is dependent upon the holding potential. (See Brown and Noble, 1969b for an application of this method of analysis in atrial muscle.)

The depolarizations which give rise to the decay tails shown in Figure 13 are of equal durations. Hence, the largest tail should correspond to the +70 mV pulse. However, this is not observed experimentally, which provides part of the evidence that the membrane currents have been altered by changes in driving force.

If such changes occur, a steady-state activation curve cannot be obtained. Nevertheless, it is important to establish the range of potentials over which the outward currents are activated. This information may be obtained in an approximate way by plotting the maximum tail amplitude at each depolarization as a function of the level (magnitude) of the depolarization. The graph shown in Figure 14 was constructed in this way. The curve was drawn by eye through the points up to +10 mV. Beyond this potential the decay tails rapidly become much smaller. From this 'composite activation curve' it is clear (i) that the activation threshold for delayed outward currents is approximately -40 mV, (ii) that the degree of activation is a steep function of potential between -30 mV and 0 mV, and (iii)

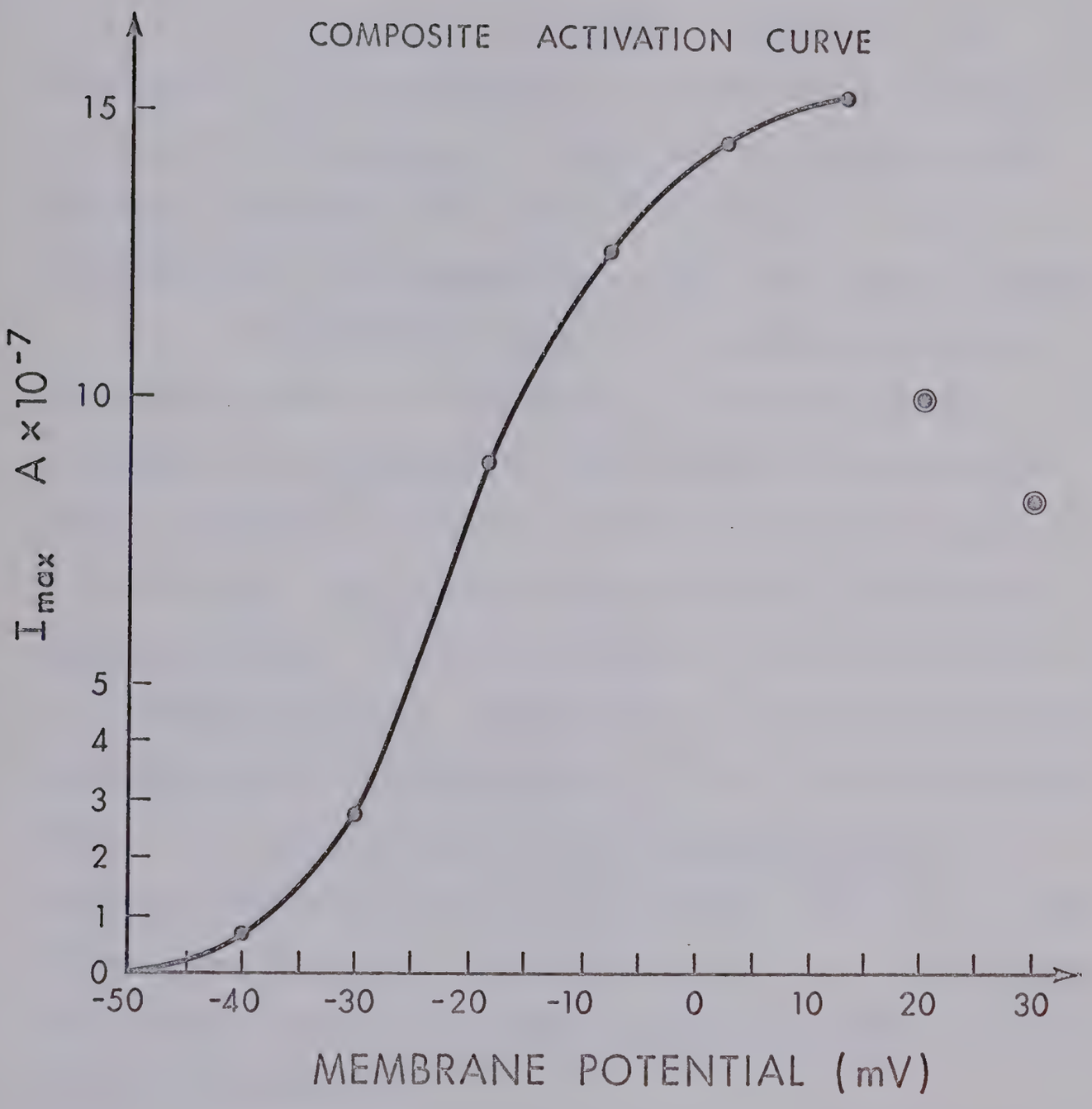

FIGURE 14: Composite 'Activation Curve'. This graph was obtained by plotting the maximum tail amplitudes at each level of depolarization shown in Figure 13. Note that the outward current is activated at about -40 mV, becomes a rather steep function of potential, and approaches a maximum at about +10 mV. The circled points indicate the decreased tail magnitudes which are thought to have resulted from extracellular concentration changes (see text).

that the currents become maximally activated at about +10 mV.

III.2 (c) TIME-DEPENDENCE OF OUTWARD CURRENTS:

In the experiment shown in Figure 13, the amplitude of the decay tails was used to describe the effect of the preceding level, or magnitude of depolarization. However, the decay tail amplitude may also be used to determine the time-dependence of the slow current changes.

Figure 15 illustrates an experiment which was designed to test the dependence of the slow outward current changes on the duration of the preceding depolarization. Thus, a holding potential was chosen from which large outward currents could be rapidly activated. A succession of depolarizations were then applied for various durations, and the decay tails which resulted from each clamp pulse were superimposed to form the family of tails shown in Figure 15B. It is apparent that each increase in clamp pulse duration activates more outward current, and that at relatively long durations (greater than 1.5 sec.) the initial rate of decrease of the decay tail is much more rapid than at shorter durations.

More quantitative information regarding the rate of decay of the positive tails can be obtained by constructing semilog plots of the decay tail magnitudes as a function of duration, for each clamp pulse. The decay tails used to construct the plots shown in Figure 16 were obtained from the same experiment as those shown in Figure 15. In this

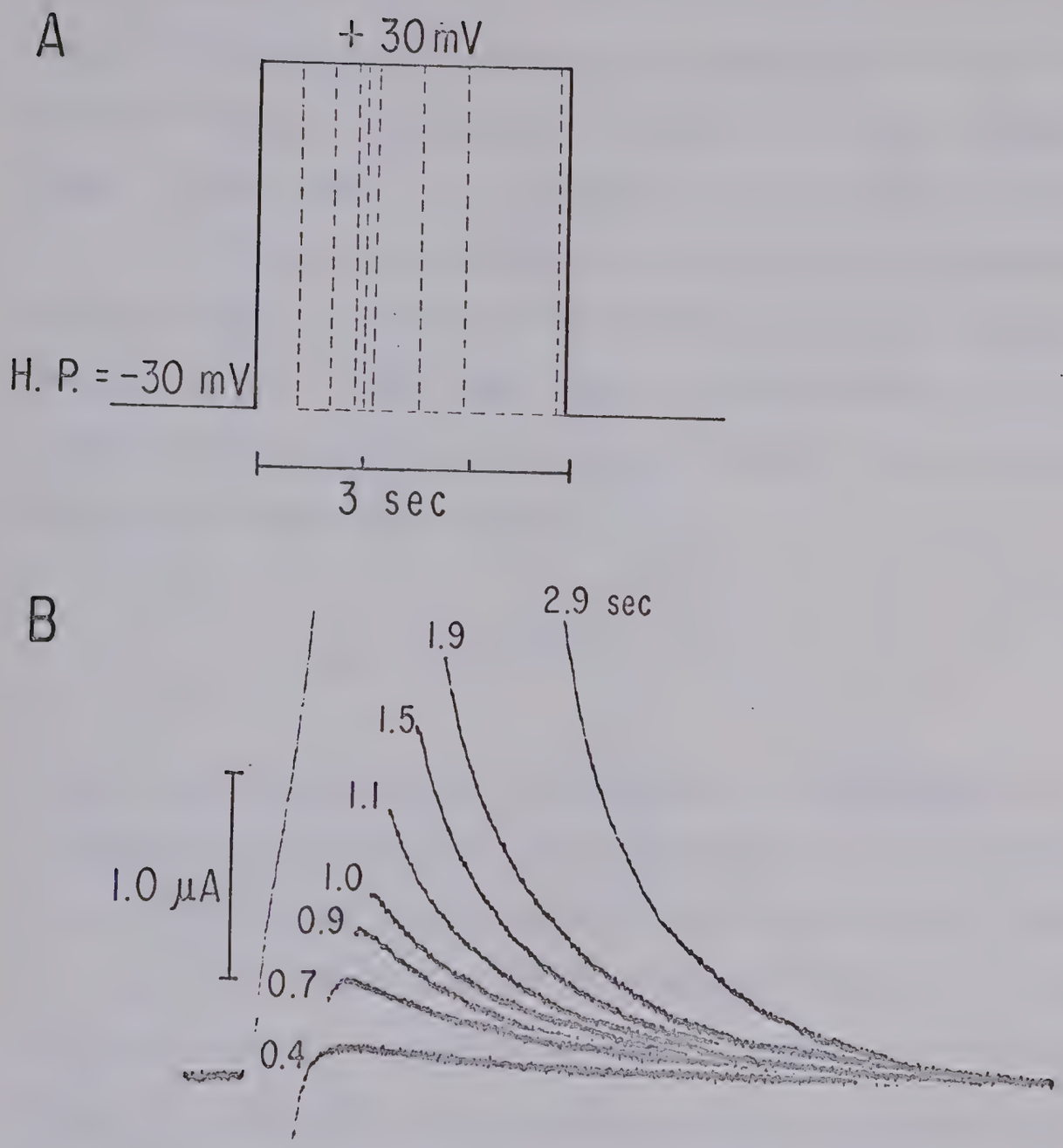

FIGURE 15: Time-dependent activation of slow outward currents. Depolarizing pulses of various durations are drawn in A, and pen recordings of decay tails are photographically superimposed in B. Labels on the decay tails indicate the duration of the preceding pulse. The partial record of current activation which is shown in B corresponds to the 2.9 sec. pulse.

case, however, a constant depolarization of +50 mV, rather than +60 mV, was applied. The decreased depolarization would be expected to decrease the magnitudes of positive tails slightly, but should not alter the time constants of decay, since these are a function of the holding potential.

Figure 15 illustrates that for depolarizations shorter than 1.5 seconds, the points may be fitted by a straight line. This means that at these durations, the quantitative relationship between current and time must be that of a simple exponential:

$$i_1 = i_{1_0} e^{-t/\tau_1}$$

where i_1, represents the current due to component 1; i_{1_0}, is the initial value of this component; τ_1, is the time constant of decay at the chosen holding potential; and t is the time. Since the holding potential was not changed between pulses, the time constant of decay for each pulse should be constant. The semilog plots corresponding to 0.8, 1.0, and 1.4 second depolarizations fulfill this prediction. In each case, the time constant is 1.9 seconds.

It is apparent, however, that this linear relationship between ln i and t is not applicable to the decay tails which follow depolarizations lasting longer than 1.4 seconds. On the basis of previous results, (Brown and Noble, 1969a; Noble and Tsien, 1969a), it might be postulated that the curves obtained from the 1.5 and 2.2

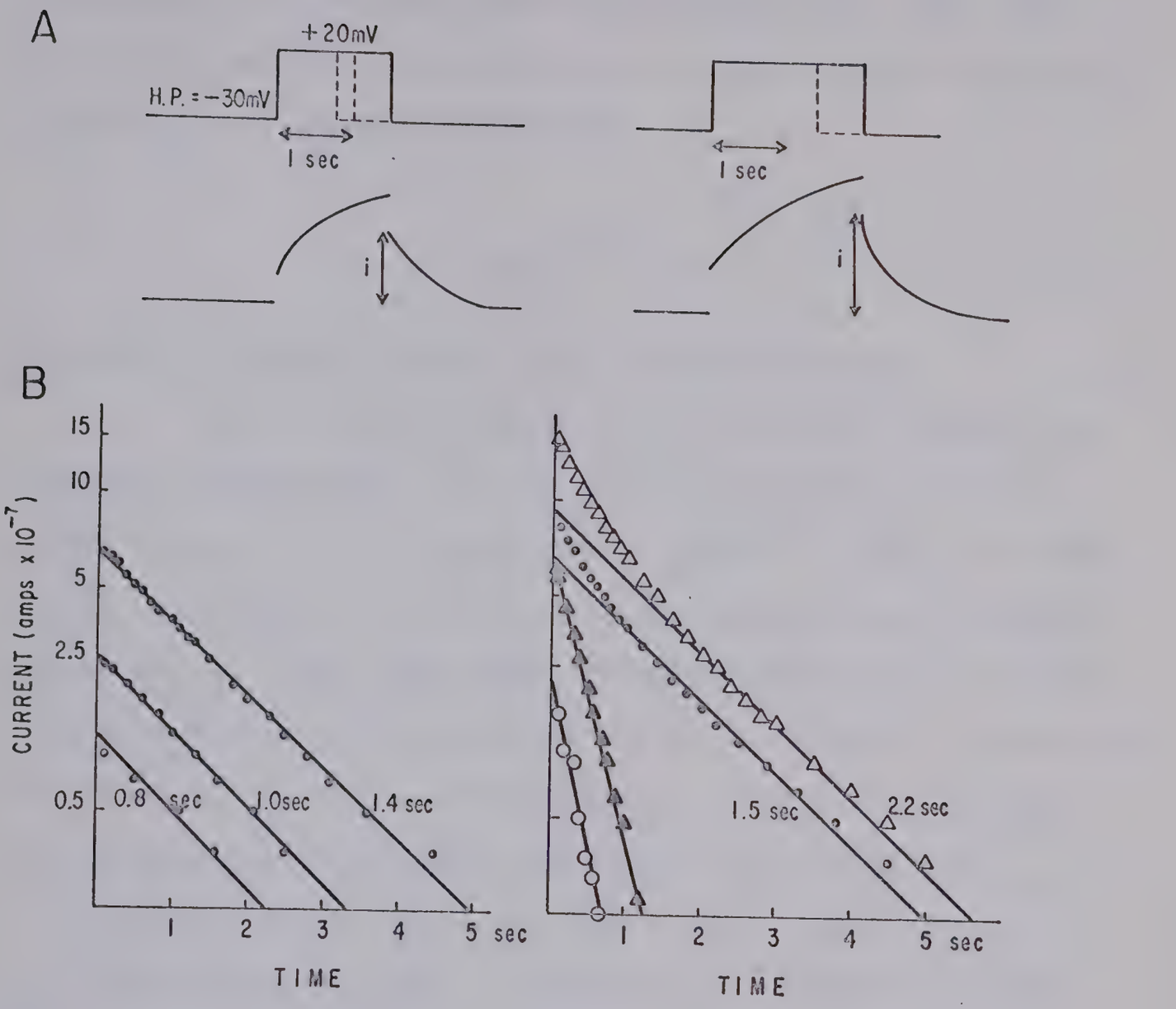

FIGURE 16: Semilog analysis of current tails following depolarizations to +20 mV lasting from 0.8 to 2.2 sec. Part A illustrates the depolarizing pulses used, and the way in which the tail analysis was done. Part B shows semilog plots obtained by graphing the decay tail magnitudes (filled circles for 0.8, 1.0, 1.4 and 1.5 sec. depolarizations, and open triangles for the 2.2 sec. depolarization) against time. The tails following depolarizations of less than 1.4 sec. were each fitted by a straight line giving a time constant of 1.9 sec. Longer duration tails were then fitted by the same straight line, and the 'fast component' (see text) was subtracted off, giving the points shown as open circles (1.5 sec. pulse) and filled triangles (2.2 sec. pulse). The time constants for the two 'fast components' were 415 msec. and 475 msec.

second depolarizations contain two exponential components of current decay. Thus, a second outward current, having a time course of decay described by

$$i_2 = i_{2_0} e^{-t/\tau_2}$$

may be activated by these longer depolarizations.

If this is the case, it is possible to obtain an indirect measurement of i_2 by using the existing semilog plot. Note, that the later points appear to form a straight line, which may be fitted by a line having a time constant equal to τ_1. This line, upon extrapolation to t=0, should supply a series of values from t=0 to t=x (where x represents the time at which all of component 2, or i_2, has decayed) which, when subtracted from the points representing i_{total}, will provide values of i_2 at each time t. Moreover, if i_2 decays exponentially, a semilog plot of the calculated i_2 values versus time should also be linear. Figure 16B (right) shows that in fact the calculated values of i_2 do fit a straight line. The time constants for these two decay tails of i_2 were 415 and 475 milliseconds.

These results, therefore, establish that two current components underlie delayed rectification in Rana catesbeiana. The slower component, i_1, may be identical with the slow component, i_{x_2}, identified by Brown and Noble (1969b) in Rana ridibunda. The time constant of the fast component, i_2, is comparable to that of the fast component

in Rana ridibunda. However, further voltage clamp analysis is needed to establish whether any further differences exist between these components.

The observation that both current components (i_1 and i_2) decay in an exponential fashion is very significant for the purpose of further analysis, since it suggests that first order kinetics control the current changes. It may be possible, therefore, to analyse the results in terms of the Hodgkin-Huxley model, in which current changes are controlled by voltage-dependent 'gates' on membrane channels. In particular, the power function of the variable controlling the degree of activation may easily be calculated.

To do this, it is necessary to plot the maximum decay tail amplitudes, obtained from the semilog plots, as a function of the duration of the preceding depolarizations. The resulting 'envelopes of tails' for the slow (i_1) and the fast (i_2) components of current change are shown in Figures 17 and 18, respectively. In each Figure it is apparent that increasing the magnitude of depolarization increases both the magnitude and the rate of activation of the outward current. However, when the duration of +50 mV or +60 mV depolarizations exceeds 3 seconds (circled points) the decay tails decrease in magnitude. This is consistent with the hypothesis that relatively long duration depolarizations may cause a sufficient amount of outward current flow to produce extracellular concentration

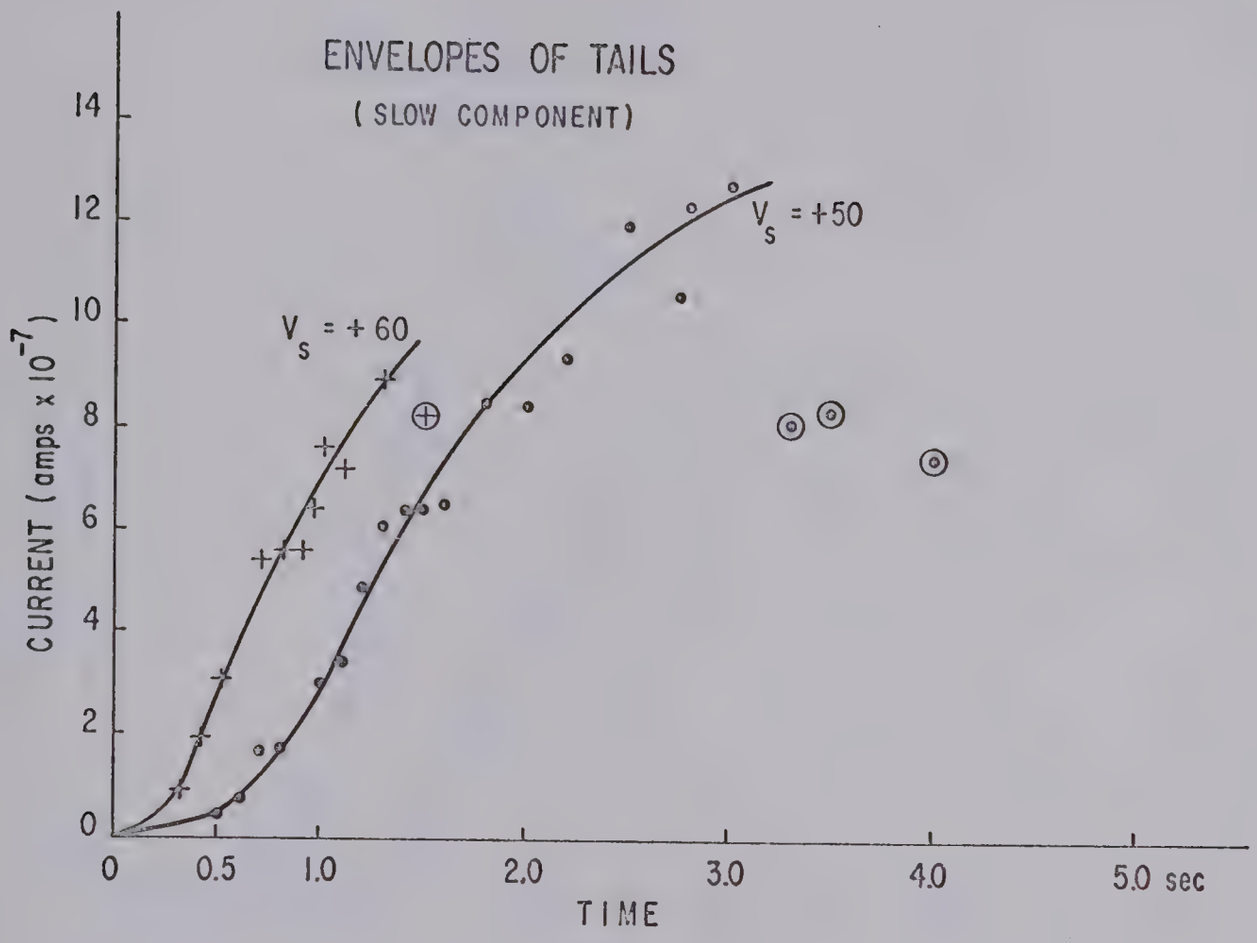

FIGURE 17: Envelopes of tails for the slow component (i_1) of current change. Note that increasing the level of depolarization increases the magnitude, and the rate of activation of the corresponding decay tails. Circled points are values which may be in error due to possible concentration changes (see text).

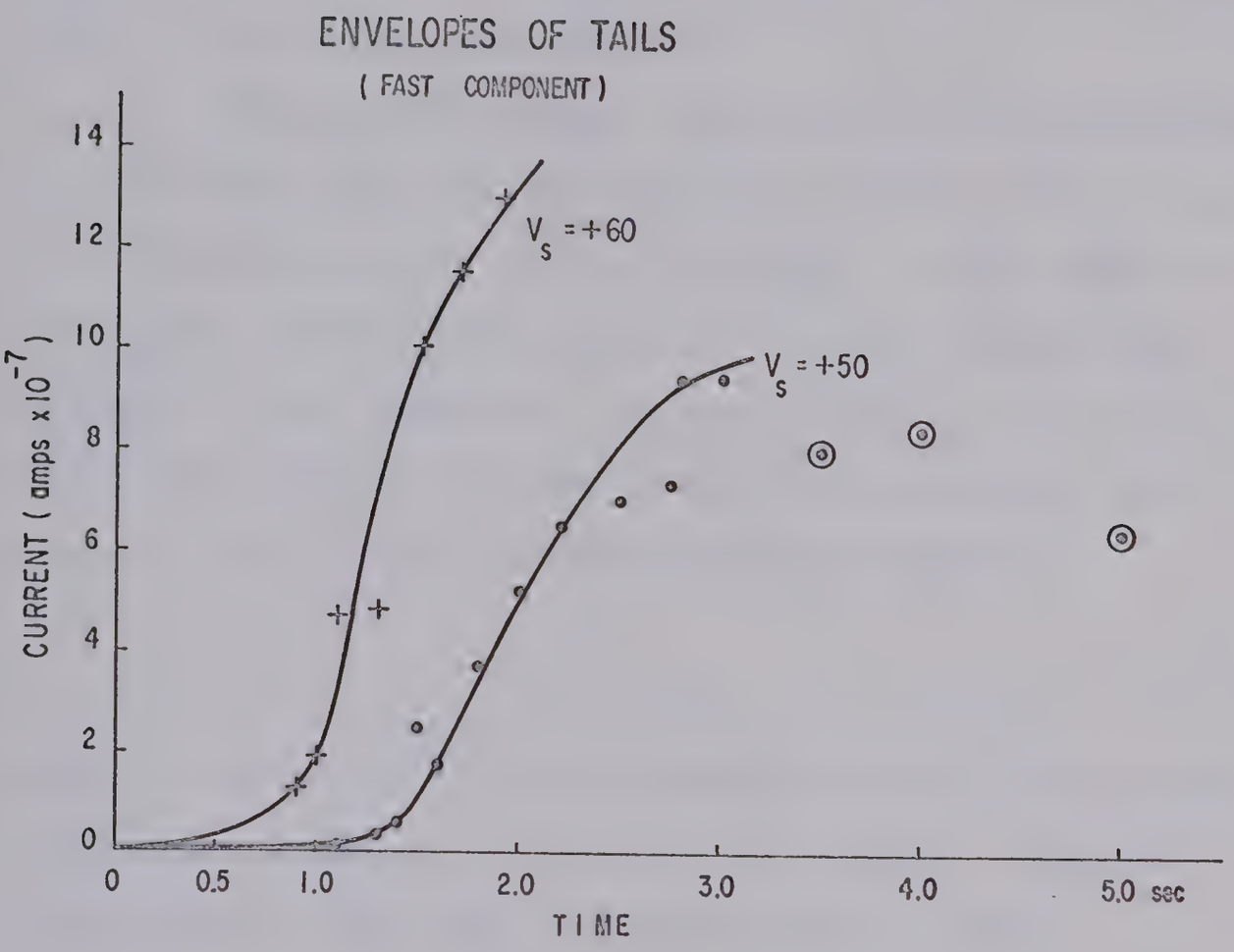

FIGURE 18: Envelopes of tails of the fast component (i_2) of current change. Note that this component is activated only after a much longer delay than the slower component. As in Figure 17, circled points indicate values which are subject to error.

changes. By comparing Figure 17 and 18 it is obvious that, for a given level of depolarization (eg. +50 mV) the slow component activates with much less delay than the fast component. In the Hodgkin-Huxley model, this delay is described by making the current change proportional to a power of the activation variable.

This model assumes that the rate of current change is controlled by a voltage-dependent, first order process, x, corresponding to a 'gating reaction' in the membrane. The 'gates' control the entry of ions into conductance channels in the membrane. For any channel to be in the conducting state all of the 'gates' must be open. The current flow, i_1, may therefore be described by

$$i \alpha x^{\gamma} \qquad \text{(I)}$$

where γ, the power of the activation process, represents the number of gates controlling the channel. Taking logarithms of both sides of expression (I) gives

$$\log i \alpha \gamma \log x \qquad \text{(II)}$$

Since x is assumed to change exponentially with time, then for small values of t, $\Delta x \alpha \Delta t$. Hence, expression (II) may be rewritten as

$$\log i \alpha \gamma \log t$$

A plot of log i versus log t should, therefore, give a straight line having a slope of γ. The values of i and t may be obtained from the envelopes of tails.

Parameters of Membrane Current Changes

Expt. Number	Holding Potential (mV)	τ_S (sec)	τ_F (msec)	γ_S	γ_F
3 - 5	-40	2.6	350-400	(+30) = 1	(+30) = 2
				(+40) = 1	(+40) = 2
3 - 8	-30	2.7	400		
3 - 9	-30	1.5	100-120		
3 - 13	-30	1.6	100-120		
3 - 22	-20	2.2	400-500	(+40) = 1	(+40) = 3
3 - 26	-30	5.6	750-800	(+20) = 1	(+20) = 1
				(+30) = 1	(+30) = 2-3
				(+40) = 1	(+40) = 2
3 - 27	-40	1.5		(+60) = 1	
4 - 29	-40	2.2	400-425	(+40) = 1	(+40) = 1-2
4 - 30	-30	1.9	400-450	(+50) = 3	(+50) = 8
				(+60) = 2	(+60) = 4

TABLE 2: τ_S and τ_F represent the respective time constants of the slow and fast components of the membrane current. γ_S and γ_F represent the powers to which the kinetic variable controlling the slow and fast current changes must be raised in order to accurately describe the observed pattern of current onset. The numbers in brackets in the γ_S and γ_F columns indicate the magnitudes of the clamp pulses which were superimposed on the holding potential. Each clamp pulse magnitude is associated with a different γ value but the time constant changes only when the holding potential is altered (see text).

Since a steady-state analysis cannot be performed, a complete Hodgkin-Huxley description of the membrane currents in Rana catesbeiana is not possible. Nevertheless, obtaining certain parameters of current change can be very useful as criteria for judging the validity of individual experiments. For example, from Table 2, it is obvious that the γ values obtained from experiment 4-30 are significantly higher than those obtained from the preceding eight experiments. This may be an indication that the preparation was not uniformly polarized in this experiment.

III.2 (d) REVERSAL POTENTIALS OF OUTWARD CURRENTS:

To extend the comparison of these results with those obtained by Brown and Noble (1969a,b), it is useful to determine the reversal potentials of both components of outward current. This may be done by performing experiments of the kind shown in Figures 19 and 20.

The preparation is first depolarized sufficiently to activate a large outward current, and is then repolarized to progressively more negative potentials. Figure 19 (left) shows that the slow component of current change reverses direction between -45 mV and -55 mV. The fast component, however, reverses at some potential negative to -85 mV. The hyperpolarizing pulses in Figure 19 (right) indicate that a small fraction of the slow component may be activated at a holding potential of -35 mV.

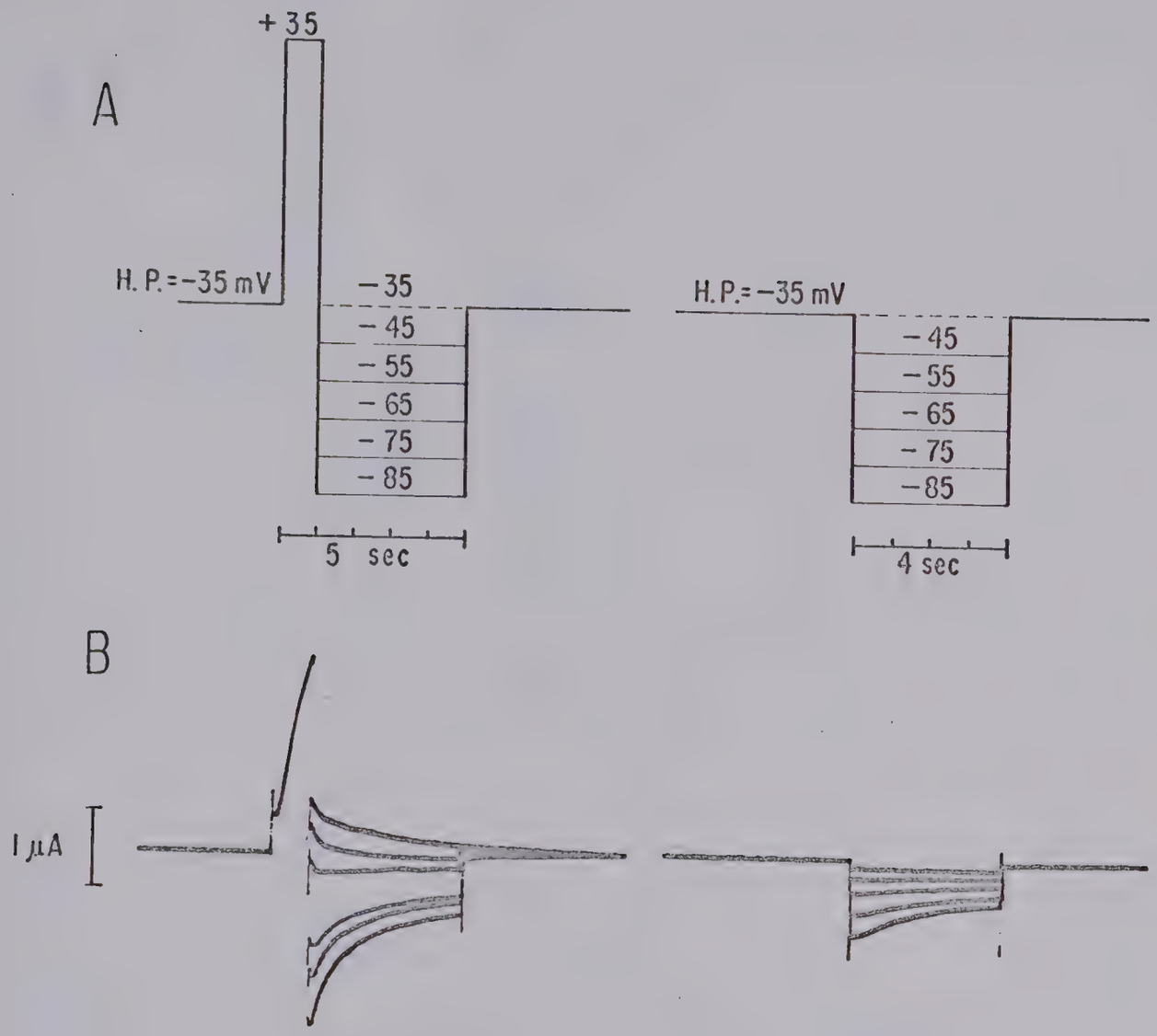

FIGURE 19: Estimate of the reversal potentials of the fast and slow components of current change. Voltage clamp pulses are drawn (A), and corresponding pen recordings of current changes are photographically superimposed (B). Both the double-pulse test (left) and the hyperpolarizations (right) indicate that the slow component reverses direction between -45 mV and -55 mV. The fast component, however, reverses at a potential more negative than -85 mV.

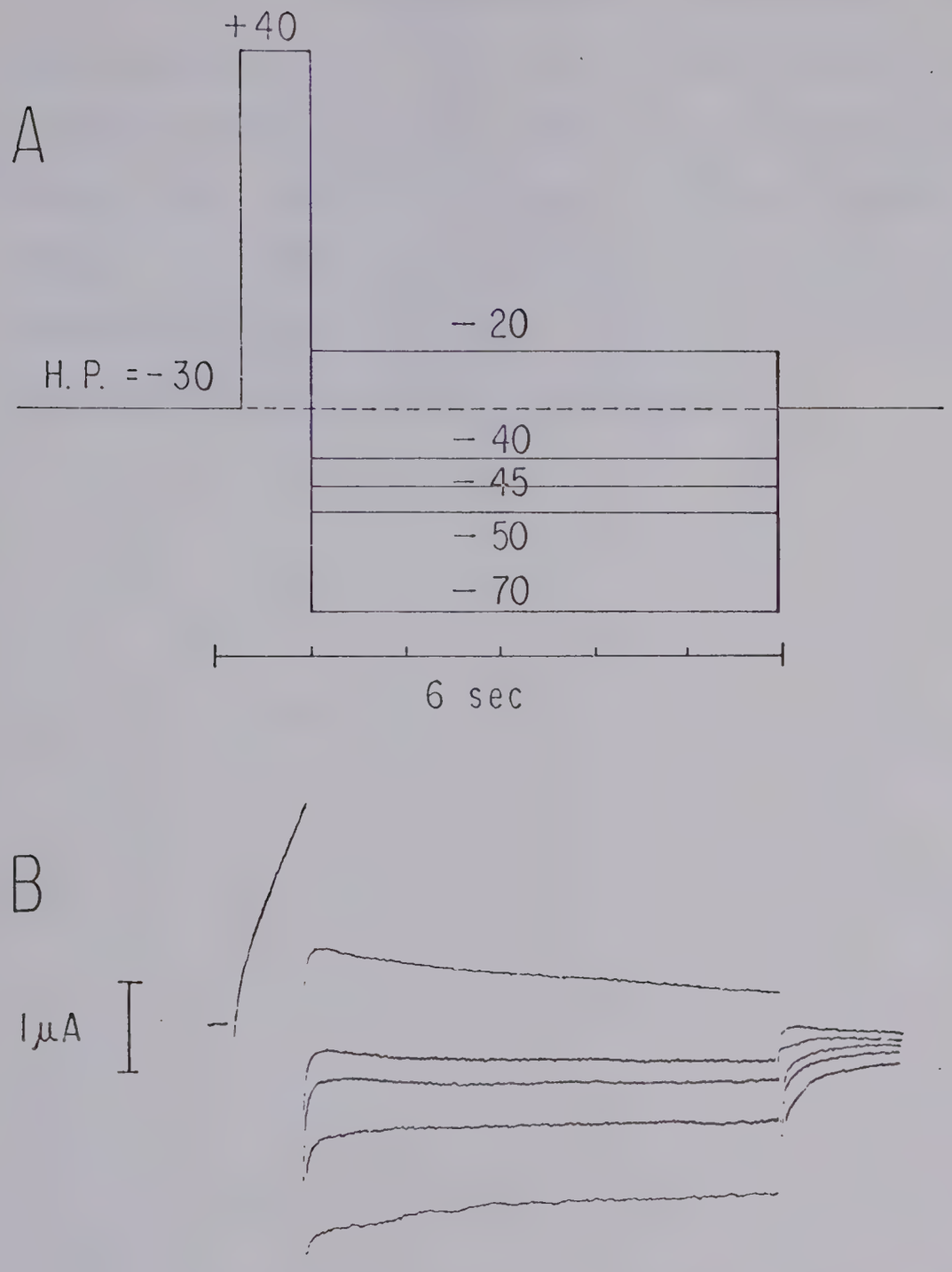

FIGURE 20: Estimate of the reversal potential for the slow component of current change. The photographically superimposed current traces show that the reversal potential is between -45 mV and -50 mV.

In the experiment shown in Figure 20, the initial depolarization has a sufficiently short duration (800 msec.) to activate only the slow component of current change. The results show that this component reverses between -45 mV and -50 mV. This reversal potential is comparable to that estimated by Brown and Noble (1969a) for the slow component of outward current in Rana ridibunda.

IV. DISCUSSION:

The quantitative studies of membrane currents reported in this thesis depend critically upon the physiological condition of the preparation. Since the experimental technique involved a tedious dissection procedure and required a fine muscle strip to be completely removed from the heart, it is possible that the preparations were in a damaged state. Several aspects of the results, however, indicate that this was not the case. Thus, the action potentials and resting potentials (measured as gap potentials) were consistently as large as those recorded from intact frog atria with intracellular microelectrodes (Glitsch, Haas, Trautwein; 1963). Moreover, it was possible to induce pacemaker activity in virtually every preparation. It is interesting to note that Rougier et al (1968,1969) rarely were able to induce pacemaker activity in their preparations. The precise reason for this is not known. However, one possibility is that the extremely narrow centre compartment (100-150 microns) in their apparatus prevented the preparation from being adequately perfused.

The effective width of the test compartment in the perfusion baths used in these experiments was approximately 300 microns. Hence, the axial voltage decrement would be greater than that in the experiments of Rougier et al. The possibility of ineffective voltage clamp control of membrane potential therefore is inherent in this technique.

Non-uniformities due to the large conductance increases which underlie the rapidly activated inward currents (Beeler and Reuter, 1970a,b) should not affect the analysis of the slower, outward currents. However, the large depolarizations that were frequently used in these experiments may have activated a sufficient amount of delayed conductance to significantly reduce the membrane space constant.

When this is the case, a substantial voltage decrement will develop between the current-passing end and the voltage-recording end of the test segment of the preparation. The feedback circuit, however, is designed to keep the membrane potential equal to the command potential at the voltage-recording end of the test gap. The increased voltage decrement therefore manifests itself as an increased depolarization at the current-passing end of the preparation. This increased depolarization then activates an additional conductance increase which further reduces the membrane space constant. Hence, the initial conductance increase is regenerative, and prevents uniform voltage control in situations where the axial voltage decrement is significant.

Since the membrane currents are voltage dependent, non-uniformity produces artifacts on the current records. In particular, the regenerative conductance increases cause the time course of the activation to be sigmoid. This may explain the sigmoid onsets of conductance observed in some of the present experiments. For example, the largest power functions

for both the slow and the fast component of current change were obtained from the same experiment (experiment 4-30; Table 2). Since analysis of results from every other experiment indicated that the slow component activates in a simple exponential fashion, this experiment is very likely to have been influenced by non-uniformity.

Therefore, it appears that the slow component of current change is controlled by a simple exponential process which may be described by first order kinetics. This result agrees with that obtained by Brown and Noble for the slow component in Rana ridibunda, and reinforces the view that the slow components in the two preparations are very similar.

However, when relatively long duration depolarizations are used to activate the membrane currents, the results become more complex. In particular, the decay tails become smaller and neither the fast nor the slow component of current change may be identified by semilog analysis. These differences have been attributed to concentration changes in the immediate vicinity of the cell membranes. In Rana catesbeiana the presence of relatively large outward currents and the restricted extracellular spaces make these 'accumulation effects' extremely difficult to avoid. In fact, it was not possible to do steady-state analysis in any of the experiments in this study.

Hence, it is not possible to clearly establish the functional significance of the two components of current

change. It is worth noting, however, that the slowly decaying component is activated sufficiently quickly and in the appropriate range of potentials to be significant during the repolarization phase of the atrial action potential. Its reversal potential of -50 mV indicates that it may also be important in the generation of pacemaker activity. In particular, it could provide a positive current whose decay may generate the pacemaker potential. The faster component of current change, however, appears to have no effect in a normal atrial action potential since it is activated only after an approximately 1 second delay. A complete reconstruction of the repolarization and pacemaker phases of the atrial action potential will require more voltage clamp experiments.

The following kinds of experiments would be interesting and useful:

(1) A metabolic blocker such as 2-4 dinitrophenol (DNP) might be used to inhibit the sodium-potassium pump. The phenomena attributed to the accumulation of potassium ions in the extracellular spaces should be enhanced after the blocker has been applied.

(2) It may be possible to construct a different perfusion bath, having a narrower centre or test gap (eg. 200 microns). This should increase the effectiveness of the potential control in the test gap. If non-uniform polarization did occur in the present experiments, comparison of these results with those obtained using the narrower test gap may reveal significant differences in the pattern of current onset and decay.

(3) A suitable pharmacological blocking agent may be able to reduce the delayed conductance sufficiently to improve the spatial uniformity of the voltage clamp. It may also reduce the extracellular concentration changes sufficiently to allow steady-state analysis. Tetraethyl-ammonium (TEA) has been shown to have this effect on myelinated nerve.

BIBLIOGRAPHY

Adrian, R.H. & Freygang, W.H. (1962). The potassium and chloride conductance of frog muscle membrane. J. Physiol. 163, 61-103.

Baldwin, K. (1968). Fine structure and electrophysiology of heart muscle cell injury. Ph.D. Thesis, University of Washington.

Barr, L., Dewey, M.M. & Berger, W. (1965). Propagation of action potentials and the structure of the nexus in cardiac muscle. J. gen. Physiol. 48, 797-823.

Beeler, G.W. & Reuter, H. (1970a). Voltage clamp experiments on myocardial fibres. J. Physiol. 207, 165-190.

Beeler, G.W. & Reuter, H. (1970b). Membrane calcium current in ventricular myocardial fibres. J. Physiol. 207, 191-209.

Brady, A.J. (1964). Physiology of the amphibian heart. In Physiology of the Amphibia, ed. Moore, A.J., Academic Press.

Brady, A.J. & Woodbury, J.W. (1960). The sodium-potassium hypothesis as the basis of electrical activity in the frog ventricle. J. Physiol. 154, 385-407.

Brown, H.F. & Noble, S.J. (1969a). Membrane currents underlying delayed rectification and pacemaker activity in frog atrial muscle. J. Physiol. 204, 717-736.

Brown, H.F. & Noble, S.J. (1969b). A quantitative analysis of the slow component of delayed rectification in frog atrium. J. Physiol. 204, 737-747.

Cole, K.S. (1949). Dynamic electrical characteristics of the squid axon membrane. Arch. Sci. Physiol., 3, 253-258.

Deck, K.A., Kern, R. & Trautwein, W. (1964). Voltage-clamp technique in mammalian cardiac fibres. Pflügers Archiv. 280, 50-62.

Glitsch, H.G., Haas, H.G. & Trautwein, W. (1965). The effect of adrenaline on the K and Na fluxes in the frog's atrium. Arch. Exp. Path. Pharmak. 250, 59-71.

Haas, H.G., Glitsch, H.G., & Kern, R. (1966). Kalium-Fluxe und Membran-potential am Froschvorhof in Abhängigkeit von der Kalium-Außen-konzentration. Pflügers Archiv. 288, 43-64.

Haas, H.G., Glitsch, H.G. & Trautwein, W. (1963). Natrium-Fluxe am Vorhof des Frosch herzens. Pflügers Archiv. 277, 36-47.

Haas, H.G., Kern, R. & Einwachter, H.M. (1970). Electrical activity and metabolism in cardiac tissue: An experimental and theoretical study. (Submitted to J. Memb. Biol.).

Hecht, H.H., Hutter, O.F. & Lywood, D.W. (1964). Voltage-current relation of short Purkinje fibres in sodium-deficient solutions. J. Physiol. 170, 5P.

Hodgkin, A.L. & Huxley, A.F. (1952). A quantitative description of membrane current and its application to conduction and excitation in nerve. J. Physiol. 117, 500-544.

Hutter, O.F. & Trautwein, W. (1956). Vagal and sympathetic effects on the pacemaker fibres in the sinus venosus of the heart. J. gen. Physiol. 39, 715-733.

Luttgau, H.C. & Niedergerke, R. (1958). The antagonism between Ca and Na ions on the frog heart. J. Physiol. 143, 486-505.

Marmot, G. (1949). Studies on the axon membrane. A new method. J. Cell. Comp. Physiol. 34, 351-382.

McAllister, R.E. & Noble, D. (1966). The time and voltage dependence of the slow outward current in cardiac Purkinje fibres. J. Physiol. 186, 632-662.

Noble, D. (1962). The voltage dependence of the cardiac membrane conductance. Biophys. J. 2, 381-393.

Noble, D. (1965). Electrical properties of cardiac muscle attributable to inward-going (anomalous) rectification. J. Cell. Comp. Physiol. 66, suppl. 2, 127-136.

Noble, D. & Tsien, R.W. (1968). The kinetics and rectifier properties of the slow potassium current in cardiac Purkinje fibres. J. Physiol. 195, 185-214.

Noble, D. & Tsien, R.W. (1969). Outward membrane currents activated in the plateau range of potentials in cardiac Purkinje fibres. J. Physiol. 200, 204-231.

Rougier, O., Vassort, G. & Stämpfli, R. (1968). Voltage clamp experiments on frog atrial heart muscle fibres with the sucrose gap technique. Pflügers Arch. ges. Physiol. 301, 91-108.

Rougier, O., Vassort, G., Garnier, D., Gargouil, Y.M. & Coraboeuf, E. (1969). Existence and role of a slow inward current during the frog atrial action potential. Pflügers Arch. ges. Physiol. 308, 91-110.

Stämpfli, R. (1945). A new method for measuring membrane potential with external electrodes. Experientia, 10, 508-509.

Stämpfli, R. (1963). Die doppelte saccharosetrennwandemethode zue messung von elektrischen membraneigen-schaften mit extracellularen electroden. Helv. Physiol. Pharmacol. Acta, 21, 189-204.

Tanaka, I. (1959). Apparent membrane resistance changes during repolarization of toad atrium. Federation Proc., 18, 156.

Toda, N. (1968). Influence of sodium ions on the membrane potential of the sinoatrial node in response to sympathetic nerve stimulation. J. Physiol. 196, 677-691.

Trautwein, W., Kuffler, S.W. & Edwards, C. (1956). Changes in membrane characteristics of heart muscle during inhibition. J. gen. Physiol. 40, 135-145.

Weidmann, S. (1951). Effect of current flow on the membrane potential of cardiac muscle. J. Physiol. 115, 227-236.

Weidmann, S. (1952). The electrical constants of Purkinje fibres. J. Physiol. 118, 348-360.

Woodbury, J.W. & Crill, W.E. (1961). On the problems of impulse conduction in the atrium. In Nervous Inhibition, ed. Florey, E. Oxford: Pergamon Press.

Woodbury, J.W. & Gordon, A.M. (1965). The electrical equivalent circuit of heart muscle. J. Cell. Physiol. 66, Suppl. 2, 35-42.